ÉCOLE POLYTECHNIQUE FÉDÉRALE DE LAUSANNE
MATHICSE
Institute of Mathematics
School of Basic Sciences

MATHICSE Technical Report
Nr. 06.2019
February 2019

A minimal stabilization procedure for isogeometric methods on trimmed geometries

A. Buffa, R. Puppi, R. Vazquez

Address: EPFL - SB – INSTITUTE of MATHEMATICS – Math
(Bâtiment MA) Station 8 - CH-1015 - Lausanne - Switzerland

A MINIMAL STABILIZATION PROCEDURE FOR ISOGEOMETRIC METHODS ON TRIMMED GEOMETRIES*

A. BUFFA [‡†], R. PUPPI [‡], AND R. VÁZQUEZ [‡†]

Abstract. Trimming is a common operation in CAD, and, in its simplest formulation, consists in removing superfluous parts from a geometric entity described via splines (a spline patch). After trimming the geometric description of the patch remains unchanged, but the underlying mesh is unfitted with the physical object. We discuss the main problems arising when solving elliptic PDEs on a trimmed domain. First we prove that, even when Dirichlet boundary conditions are weakly enforced using Nitsche's method, the resulting method suffers lack of stability. Then, we develop novel stabilization techniques based on a modification of the variational formulation, which allow us to recover well-posedness and guarantee accuracy. Optimal a priori error estimates are proven, and numerical examples confirming the theoretical results are provided.

Key words. isogeometric analysis, trimming, unfitted finite element, finite element methods, stabilized methods

AMS subject classifications. 65N12, 65N15, 65N30, 65N85

1. Introduction. Complex models are processed within Computer Aided Design (CAD) tools where several geometric manipulations are possible. Geometries are described as collection of their boundary surfaces, often defined as tensor-product splines or NURBS, and during the design process these surfaces can be joined, intersected or simply superflous parts can be cut away. All these Boolean operations act on the original surfaces through a common procedure of trimming. When the superfluous surface areas are cut away, the visualization of the resulting surface changes, while its mathematical description does not. This description of the geometry is called "boundary representation" (B-rep), and we defer the interested reader to [33, 40], or to the recent review [29] and references therein. This representation is clearly not well suited for the simulation of partial differential equations (PDEs).

Several efforts have been undertaken in the last years to improve the usability of CAD geometries in the solution of PDEs, especially after the advent of Isogeometric Analysis (IGA) [14, 25]. Indeed, IGA has been a tremendous success since 2005 with a wide range of applications (see for instance [24]), and it is becoming a mature method: its mathematical analysis is now well understood [4], fast assembly and solvers exist today [1, 37] and strategies for adaptive refinement with a sound mathematical theory are now available, see [5] and the references therein. The geometric modelling community has also provided important inputs to this scientific challenge [36], and new strategies to define geometric entities through the volume they occupy instead of their boundaries are now emerging, for instance, the volumetric representations (V-reps) proposed in [30]. On the other hand, trimming remains a main tool for the design of complex models via Boolean operations, and basically all developments of IGA described above rely on strong requirements on the underlying geometric models

*Submitted.

Funding: The authors were partially supported by ERC AdG project CHANGE n. 694515, by MIUR PRIN project "Metodologie innovative nella modellistica differenziale numerica", and by Istituto Nazionale di Alta Matematica (INdAM).

† Istituto di Matematica Applicata e Tecnologie Informatiche "Enrico Magenes" del CNR, Pavia, Italy.

‡Chair of Modelling and Numerical Simulation, Institute of Mathematics, École Polytechnique Fédérale de Lausanne, Lausanne, Switzerland (annalisa.buffa@epfl.ch, riccardo.puppi@epfl.ch, rafael.vazquez@epfl.ch).

and, in general, do not support trimmed geometric entities. The aim of this paper is to contribute to the design of isogeometric methods that robustly support trimming in the geometric description of the computational domain, and do not require the construction of a global re-parametrization (meshing).

The two main issues arising when dealing with trimmed geometries are the presence of elements unfitted with the boundary, making the research for efficient quadrature rules and the stable imposition of boundary conditions a challenge, and the existence of basis functions whose support has been cut, affecting the conditioning of the related linear system. In this regard, ideas from fictitious domain and immersed boundary approaches in the FEM literature can be adapted to the IGA setting, and the related engineering literature includes (but is not limited to) the pioneering works regarding the integration with CAD and numerical quadrature [31, 43], the shell analysis on geometric models with B-reps [7, 32], and the finite cell method combined with IGA [15, 35, 38, 44]. Concerning the lack of stability, we should mention stabilizations based on extrapolation [23, 28], and the Cut-IGA method proposed in [26], which is related to the many contributions of Cut-FEM and ghost penalty methods [10, 11, 12, 13, 21].

We now describe the simplified mathematical setting. Let $\Omega_0 \subseteq \mathbb{R}^d$ (here $d = 2, 3$) be a domain described by a bijective spline map $\mathbf{F} : (0,1)^d \to \Omega_0$, i.e., a patch in the isogeometric terminology, and let $\Omega_1, \dots \Omega_N$ be Lipschitz regular domains in $\mathbb{R}^d$. We assume that $\bigcup_{i=1}^N \overline{\Omega}_i$ are to be cut away from Ω_0 and that our computational domain reads:

$$\Omega = \Omega_0 \setminus \bigcup_{i=1}^{N} \overline{\Omega}_i. \tag{1.1}$$

After trimming the mathematical description of the domain remains unchanged, that is, the elements and basis functions fit the boundary of Ω_0 instead of that of Ω. In this paper, we focus on a simple Poisson problem, with weakly imposed boundary conditions, on the domain Ω described above. First of all, we discuss the difference between bad matrix conditioning and lack of stability. The first one can be improved by modifying the chosen basis (preconditioning), while the second one needs to act on the bilinear form directly.

Regarding the lack of stability, we propose a minimal stabilization technique, inspired by [22], that acts only on those cut elements that affect stability. For example, in the case of a Neumann condition on the trimmed boundary, no stabilization is needed. Our stabilization is parameter free, and its computation requires only local projections at the element level, and only for "bad" cut elements. For the stabilization we follow a "local approach" (according to the review paper [29]), i.e. we modify the analysis, rather than the geometry, in order to be able to face the challenges arising from trimming. We present two different versions of the stabilization technique. The first one is a projection in the parametric domain, that is easier to implement from the numerical point of view, but suboptimal. The second one is a projection-based stabilization performed directly on the physical domain, which allows us to recover optimal a priori error estimates.

Concerning the bad conditioning of the matrix, we show numerical evidence that a rescaling of the stiffness matrix seems to consistently resolve the issue. However, the analysis on the linear algebra side is not presented, as it is beyond the scope of this work.

The document is organized as follows. Section 2 presents an overview of isoge-

ometric analysis in trimmed domains. In Section 3 we set the model problem, and explain the main challenges we need to face, namely integration, conditioning and numerical stability of the associated linear system. After having explained in detail in Section 4 the causes for the lack of stability of the simple Nitsche's formulation, in Section 5 we present our new stabilization technique. Two possible constructions of the stabilization operator are suggested and analysed in Section 6, and error estimates are provided in Section 7. Finally, we conclude by showing some numerical examples, obtained using the MATLAB library GeoPDEs [42], confirming the theoretical results.

2. Isogeometric analysis on trimmed domains.

2.1. The univariate case. For a more detailed introduction about isogeometric analysis, see for instance the review article [4]. Given two positive integers p and n, we say that $\Xi := \{\xi_1, \dots, \xi_{n+p+1}\}$ is a *p-open knot vector* if

$$\xi_1 = \cdots = \xi_{p+1} < \xi_{p+2} \leq \cdots \leq \xi_n < \xi_{n+1} = \cdots = \xi_{n+p+1}.$$

We assume $\xi_1 = 0$ and $\xi_{n+p+1} = 1$. We also introduce $Z := \{\zeta_1, \dots, \zeta_N\}$, the set of *breakpoints*, or knots without repetitions, which forms a partition of the unit interval $(0, 1)$. Note that

$$\Xi = \{\underbrace{\zeta_1, \dots, \zeta_1}_{m_1 \text{ times}}, \underbrace{\zeta_2, \dots, \zeta_2}_{m_2 \text{ times}}, \dots, \underbrace{\zeta_N, \dots, \zeta_N}_{m_N \text{ times}}\},$$

where $\sum_{i=1}^{N} m_i = n+p+1$. Moreover, we assume $m_j \leq p$ for every internal knot and we denote $I_i := (\zeta_i, \zeta_{i+1})$ and its measure $h_i := \zeta_{i+1} - \zeta_i$, $i = 1, \dots, N-1$.

We denote as $\widehat{B}_{i,p} : [0, 1] \to \mathbb{R}$ the i-th *B-spline*, $1 \leq i \leq n$, obtained using the Cox-de Boor formula, see for instance [4]. Moreover, let $S_p(\Xi) = \text{span}\{\widehat{B}_{i,p} : 1 \leq i \leq n\}$ the vector space of univariate splines of degree p. $S_p(\Xi)$ can also be characterized as the space of piecewise polynomials of degree p with $k_j := p - m_j$ continuous derivatives at the breakpoints ζ_j, $1 \leq j \leq N$ (Curry-Schoenberg theorem).

The following local quasi-uniformity assumption is classical in the IGA literature [4].

ASSUMPTION 2.1. *The partition defined by the knots $\zeta_1, \dots, \zeta_N$ is locally quasi-uniform, that is, there exists a constant $C \geq 1$ such that the mesh sizes $h_i = \zeta_{i+1} - \zeta_i$ satisfy the relation*

$$C^{-1} \leq \frac{h_i}{h_{i+1}} \leq C \qquad \forall\ 1 \leq i \leq N-2.$$

Remark 2.2. Following [9], Assumption 2.1 could be weakened.

Given an interval $I_j = (\zeta_j, \zeta_{j+1}) = (\xi_i, \xi_{i+1})$, we define its *support extension* $\widetilde{I}_j$ as

$$\widetilde{I}_j := \text{int} \bigcup \{\text{supp}(\widehat{B}_{k,p}) : \text{supp}(\widehat{B}_{k,p}) \cap I_j \neq \emptyset, 1 \leq k \leq n\} = (\xi_{i-p}, \xi_{i+p+1}).$$

2.2. The multivariate case. Let d be the space dimension. Assume that $n_l \in \mathbb{N}$, $p_l \in \mathbb{N}$, $\Xi_l = \{\xi_{l,1}, \dots, \xi_{l,n_l+p_l+1}\}$ and $Z_l = \{\zeta_{l,1}, \dots, \zeta_{l,N_l}\}$ are given for every $1 \leq l \leq d$. We set the degree $\mathbf{p} := (p_1, \dots, p_d)$ and $\boldsymbol{\Xi} := \Xi_1 \times \cdots \times \Xi_d$. Note that the breakpoints of Z_l form a Cartesian grid in the *parametric domain* $\widehat{\Omega}_0 = (0, 1)^d$. We define the *parametric Bézier mesh*

$$\widehat{\mathcal{M}}_0 = \{Q_{\mathbf{j}} = I_{1,j_1} \times \cdots \times I_{d,j_d} : I_{l,j_l} = (\zeta_{l,j_l}, \zeta_{l,j_l+1}) : 1 \leq j_l \leq N_l - 1\},$$

where each $Q_{\mathbf{j}}$ is called *Bézier element*. Let $\mathbf{I} := \{\mathbf{i} = (i_1, \dots, i_d) : 1 \le i_l \le n_l\}$ be a set of multi-indices. For each $\mathbf{i} = (i_1, \dots, i_d)$, we define the local knot vector

$$\boldsymbol{\Xi}_{\mathbf{i},\mathbf{p}} = \Xi_{i,p_1} \times \cdots \times \Xi_{i_d,p_d},$$

which allows us to define the set of *multivariate B-splines*

$$\{\widehat{B}_{\mathbf{i},\mathbf{p}}(\zeta) = \widehat{B}_{i_1,p_1}(\zeta_1) \dots \widehat{B}_{i_d,p_d}(\zeta_d) : \mathbf{i} \in \mathbf{I}\}.$$

Moreover, for a generic Bézier element $Q_j \in \widehat{\mathcal{M}}$, we define its *support extension*

$$\widetilde{Q}_j = \widetilde{I}_{1,j_1} \times \cdots \times \widetilde{I}_{d,j_d},$$

where $\widetilde{I}_{l,j_l}$ is the univariate support extension of the univariate case defined above.

The *multivariate spline space* in $\widehat{\Omega}$ is defined as

$$S_{\mathbf{p}}(\boldsymbol{\Xi}) = \operatorname{span}\{\widehat{B}_{\mathbf{i},\mathbf{p}}(\zeta) : \mathbf{i} \in \mathbf{I}\},$$

which can be also seen as the space of piecewise multivariate polynomials of degree $\mathbf{p}$ and with regularity across the Bézier elements given by the knots multiplicities. Note that $S_{\mathbf{p}}(\boldsymbol{\Xi}) = \bigotimes_{l=1}^{d} S_{p_l}(\Xi_l)$.

Remark 2.3. What has been said so far can be easily generalized to the case of Non-Uniform Rational B-Splines (NURBS) basis functions. See for instance [14].

2.3. Parametrization, mesh and approximation space for trimming domains. Let $\Omega_0 \subset \mathbb{R}^d$ be the original domain before trimming. We assume that there exists a map $\mathbf{F} \in \left(S_{\mathbf{p}^0}(\boldsymbol{\Xi}^0)\right)^d$ such that $\Omega_0 = \mathbf{F}(\widehat{\Omega}_0)$, for given degree vector $\mathbf{p}^0$ and knot vector $\boldsymbol{\Xi}^0$. We define the (physical) *Bézier mesh* as the image of the elements in $\widehat{\mathcal{M}}_0$ through $\mathbf{F}$:

$$\mathcal{M}_0 := \{K \subset \Omega : K = \mathbf{F}(Q), Q \in \widehat{\mathcal{M}}_0\}.$$

See for instance Figure 1. To prevent the existence of singularities in the parametrization we make the following assumption.

ASSUMPTION 2.4. *The parametrization* $\mathbf{F} : \widehat{\Omega}_0 \to \Omega_0$ *is bi-Lipschitz. Moreover,* $\mathbf{F}|_{\overline{Q}} \in C^\infty(\overline{Q})$ *for every* $Q \in \widehat{\mathcal{M}}_0$ *and* $\mathbf{F}^{-1}|_{\overline{K}} \in C^\infty(\overline{K})$ *for every* $K \in \mathcal{M}_0$.

Some consequences of Assumption 2.4 are the following.

1. $h_Q \approx h_K$, i.e. $\exists\, C_1 > 0, C_2 > 0$ such that $C_1 h_K \le h_Q \le C_2 h_K$;
2. $\exists\, C > 0$ such that, $\forall\, Q \in \widehat{\mathcal{M}}$ such that $\mathbf{F}(Q) = K$, it holds $\|D\mathbf{F}\|_{L^\infty(Q)} \le C$ and $\left\|D\mathbf{F}^{-1}\right\|_{L^\infty(K)} \le C$;
3. $\exists\, C_1 > 0, C_2 > 0$ such that $\quad C_1 \le |\det(D\mathbf{F}(\widehat{\mathbf{x}}))| \le C_2$, for all $\widehat{\mathbf{x}} \in \widehat{\Omega}_0$.

Let $\widehat{V}_h = S_{\mathbf{p}}(\boldsymbol{\Xi})$ be a refinement of $S_{\mathbf{p}^0}(\boldsymbol{\Xi}^0)$ and define

$$V_h = \operatorname{span}\{B_{\mathbf{i},\mathbf{p}}(\mathbf{x}) := \widehat{B}_{\mathbf{i},\mathbf{p}} \circ \mathbf{F}^{-1}(\mathbf{x}) : \mathbf{i} \in \mathbf{I}\},$$

where $\{\widehat{B}_{\mathbf{i},\mathbf{p}} : \mathbf{i} \in \mathbf{I}\}$ is a basis for $\widehat{V}_h$. Note that throughout this document C will denote generic constants that may change at each occurrence, but that are always independent of the local mesh size.

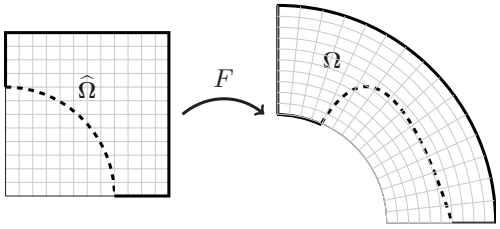

Fig. 1: On the left we see the trimmed parametric domain $\widehat{\Omega}$ and, on the right, the physical one.

3. The isogeometric formulation. At this point we suppose to trim Ω_0 as explained in (1.1), for simplicity, with $N = 1$, i.e. the new domain is $\Omega = \Omega_0 \setminus \overline{\Omega}_1$ and we assume that Ω is a sufficiently regular domain of $\mathbb{R}^d$. We denote the trimming curve as $\Gamma_{trim} = \partial\Omega \cap \partial\Omega_1$. Let us consider the Poisson equation as model problem. Given $f \in L^2(\Omega)$, $g_D \in H^{\frac{1}{2}}(\Gamma_D)$ and $g_N \in H^{-\frac{1}{2}}(\Gamma_N)$, find $u : \Omega \to \mathbb{R}$ such that

$$\begin{cases} -\Delta u = f & \text{in } \Omega \\ u = g_D & \text{on } \Gamma_D \\ \dfrac{\partial u}{\partial n} = g_N & \text{on } \Gamma_N, \end{cases} \tag{3.1}$$

where $\Gamma_D \cup \Gamma_N = \Gamma =: \partial\Omega$ and $\mathring{\Gamma}_D \cap \mathring{\Gamma}_N = \emptyset$, and $\boldsymbol{n}$ is the outward unit normal to Γ. Observe that, in general, $\Gamma_{trim} \cap \Gamma_D \neq \emptyset$.

Let us now develop and extend the notation introduced in Section 2, to adapt it to trimmed domains.

The approximation space on the trimmed domain Ω is

$$\widetilde{V}_h = \operatorname{span}\{B_{\mathbf{i},\mathbf{p}}\big|_\Omega : \mathbf{i} \in \mathbf{I}\},$$

and we set $N_h := \dim(\widetilde{V}_h)$. The new parametric Bézier mesh is

$$\widehat{\mathcal{M}} = \{Q \in \widehat{\mathcal{M}}_0 : Q \cap \widehat{\Omega} \neq \emptyset\},$$

where $\widehat{\Omega} = \mathbf{F}^{-1}(\Omega)$. The physical mesh is

$$\mathcal{M} = \{\mathbf{F}(Q) : Q \in \widehat{\mathcal{M}}\}.$$

We denote the set of Bézier elements cut by the trimming curve as

$$\mathcal{G}_h = \{K \in \mathcal{M} : \overline{K} \cap \Gamma_{trim} \neq \emptyset\}$$

and the extended computational domain

$$\Omega_\tau = \operatorname{int} \bigcup_{K \in \mathcal{M}} \overline{K}.$$

For every $K \in \mathcal{M}$, let $h_K := \operatorname{diam}(K)$, $h_{\max} := \max_{K \in \mathcal{M}} h_K$ and $h_{\min} := \min_{K \in \mathcal{M}} h_K$. We define $\mathsf{h} : \Omega \to \mathbb{R}^+$ to be the piecewise constant mesh-size function of $\mathcal{M}$ given by $\mathsf{h}\big|_K := h_K$.

First of all, we make an assumption on how the mesh is cut by the boundary.

ASSUMPTION 3.1. *There exists $C > 0$ such that, $\forall\ h > 0$, $\forall\ K \in \mathcal{M}$, it holds* $\mathrm{meas}_{d-1}(\Gamma_K) \leq C h_K^{d-1}$, *where* $\Gamma_K := \Gamma_D \cap \overline{K} \neq \emptyset$.

We denote as $\widehat{\Gamma}_D := \mathbf{F}^{-1}(\Gamma_D)$ and as $\widehat{\boldsymbol{n}}$ its outward unit normal.

Since the point is to avoid a reparametrization and a remeshing of the trimmed domain, it is natural to see the analogy with fictitious domain methods, where the physical domain, with a possibly complicated topology, is immersed into a simpler, but unfitted, background mesh. Similarly to fictitious domain methods, we need to be able to impose essential boundary conditions when the mesh is not fitted with boundary. Following [19, 39], we decide to employ Nitsche's method, which in its symmetric form reads as follows.

Find $u_h \in \widetilde{V}_h$ such that

$$\begin{aligned}\int_\Omega \nabla u_h \cdot \nabla v_h - \int_{\Gamma_D} \frac{\partial u_h}{\partial n} v_h - \underbrace{\int_{\Gamma_D} u_h \frac{\partial v_h}{\partial n}}_{\text{symmetry}} + \underbrace{\beta \int_{\Gamma_D} \mathsf{h}^{-1} u_h v_h}_{\text{stability}} \\ = \int_\Omega f v_h + \int_{\Gamma_N} g_N v_h \underbrace{- \int_{\Gamma_D} g_D \frac{\partial v_h}{\partial n} + \beta \int_{\Gamma_D} \mathsf{h}^{-1} g_D v_h}_{\text{consistency}},\end{aligned} \tag{3.2}$$

where $\beta > 0$ is a penalization parameter.

We define

$$a_h(u_h, v_h) := \int_\Omega \nabla u_h \cdot \nabla v_h - \int_{\Gamma_D} \frac{\partial u_h}{\partial n} v_h - \int_{\Gamma_D} u_h \frac{\partial v_h}{\partial n} + \beta \int_{\Gamma_D} \mathsf{h}^{-1} u_h v_h.$$

Remark 3.2. Notice that

- the stiffness matrix associated to (3.2) is symmetric and positive definite provided β is large enough;
- the condition number of the matrix increases with β;
- the weak form is consistent with the problem, in the sense that a sufficiently regular solution to (3.2) also solves the strong problem (3.1).

As evident in the literature the formulation (3.2) on a trimmed domain needs special care as:

- it can suffer from stability problems (see CUT-FEM for the finite element case: [10, 11, 13, 21]).
- an integration strategy is needed to compute the matrix contribution of the cut elements.
- the problem may suffer from conditioning issues [17].

Our main goal is to provide a minimal stabilization to make formulation (3.2) uniformly well-posed with respect to the mesh-size.

4. Stability. Firstly, we need to clarify what we actually mean by "stability" of the discrete variational problem (3.2). Problem (3.2) is stable if the bilinear form $a_h(\cdot,\cdot)$ is bounded and coercive with respect to a suitable norm.

We introduce the following mesh-dependent scalar product

$$(u_h, v_h)_{1,h,\Omega} := \int_\Omega \nabla u_h \cdot \nabla v_h + \int_{\Gamma_D} \mathsf{h}^{-1} u_h v_h,$$

which induces the discrete norm

$$\|u_h\|^2_{1,h,\Omega} := \|\nabla u_h\|^2_{L^2(\Omega)} + \left\|\mathsf{h}^{-\frac{1}{2}} u_h\right\|^2_{L^2(\Gamma_D)}. \tag{4.1}$$

PROPOSITION 4.1. *If for all $K \in \mathcal{G}_h$ we have $\Gamma_K = \emptyset$, then problem (3.2) is well-posed, i.e., $a_h(\cdot,\cdot)$ is continuous and coercive with respect to the norm (4.1).*

Instead, if there exists $K \in \mathcal{G}_h$ such that $\Gamma_K \neq \emptyset$, when looking at the continuity of the bilinear form, we need to estimate

$$\int_{\Gamma_K} \frac{\partial u_h}{\partial n} v_h \leq \left\|\mathsf{h}^{\frac{1}{2}} \frac{\partial u_h}{\partial n}\right\|_{L^2(\Gamma_K)} \left\|\mathsf{h}^{-\frac{1}{2}} v_h\right\|_{L^2(\Gamma_K)}, \qquad \forall\, v_h \in \widetilde{V}_h, \forall\, K \in \mathcal{M}.$$

In particular, we would like the following estimate to hold

$$\left\|\mathsf{h}^{\frac{1}{2}} \frac{\partial v_h}{\partial n}\right\|_{L^2(\Gamma_K)} \leq C \|\nabla v_h\|_{L^2(\Omega \cap K)} \qquad \forall\, v_h \in \widetilde{V}_h, \tag{4.2}$$

where $C > 0$ is a constant not depending on K or $K \cap \Omega$. However, that inequality does not hold in general, which implies that the continuity and coercivity of problem (3.2) cannot be guaranteed. Indeed, let us show the lack of stability with a numerical example.

Let us consider $\Omega_0 = (0,1)^2$ and as trimmed domain $\Omega = (0,1) \times (0, \frac{3}{4} + \varepsilon)$, $\varepsilon > 0$, as shown in Figure 2. We take as reference solution $u_{\text{ex}}(x,y) = \sin(\pi x) + \sin(\pi y)$, $h = \frac{1}{32}$ and, as basis functions, B-splines of degree $p = 3$ and of class C^2 at the internal knots.

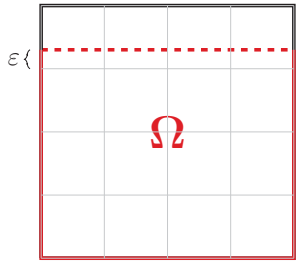

Fig. 2: Numerical experiment to test the stability of the variational formulation with respect to the mesh-boundary position. The trimmed domain is $\Omega = (0,1) \times (0, \frac{3}{4} + \varepsilon)$.

In order to check the robustness of the formulation (3.2) with respect to the parameter ε, we study the following generalized eigenvalue problem [16, 18].

Find $u_h \in \widetilde{V}_h \setminus \{0\}$ and $\lambda_h \in \mathbb{R}$ such that

$$a_h(u_h, v_h) = \lambda_h (u_h, v_h)_{1,h,\Omega} \qquad \forall\, v_h \in \widetilde{V}_h. \tag{4.3}$$

Up to re-ordering, the solution gives eigenvalues

$$\lambda_h^1 \leq \lambda_h^2 \leq \cdots \leq \lambda_h^{N_h},$$

where

$$\lambda_h^1 = \frac{a_h(u_1^h, u_1^h)}{\|u_1^h\|^2_{1,h,\Omega}} \geq \alpha, \qquad \lambda_h^{N_h} = \frac{a_h(u_{N_h}^h, u_{N_h}^h)}{\|u_{N_h}^h\|^2_{1,h,\Omega}} \leq M,$$

where $\alpha > 0$ and $M > 0$ represent, respectively, the coercivity and continuity constants. The goal is to show that it does not exist $\beta > 0$, independent of the cutting, such that $a_h(\cdot,\cdot)$ is continuous and coercive with respect to $\|\cdot\|_{1,h,\Omega}$.

Actually, we verify that the spectrum of (4.3) strongly depends on ε. In Figure 3 we can see, in detail, the dependence of the spectrum of (4.3) on the magnitude of ε. In particular, the absolute values of the smallest and largest eigenvalues of (4.3) go to infinity as ε goes to 0, implying that the discrete formulation (3.2) is not stable.

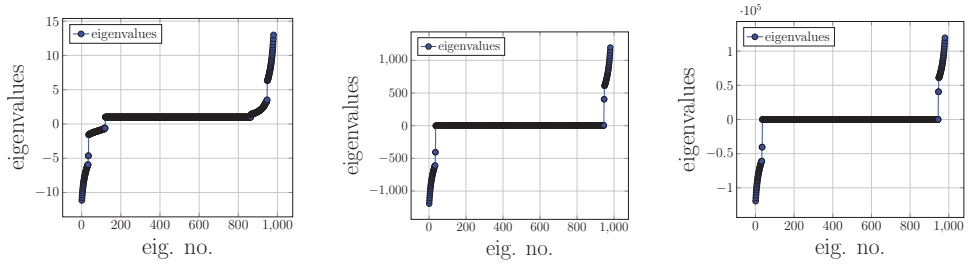

(a) Spectrum with $\varepsilon = 10^{-3}$. Magnitude of the maximum eigenvalue $\sim 10^1$.

(b) Spectrum with $\varepsilon = 10^{-7}$. Magnitude of the maximum eigenvalue $\sim 10^3$.

(c) Spectrum with $\varepsilon = 10^{-11}$. Magnitude of the maximum eigenvalue $\sim 10^5$.

Fig. 3: Generalized eigenvalues of (4.3) for different values of ε.

At this point, in order to be able to deal with a well-posed, hence stable, problem we want to find a way to improve the continuity bound of $a_h(\cdot,\cdot)$, in particular to find a trace inequality, similar to (4.2), where the constant does not depend on how the boundary intersects the mesh [22].

LEMMA 4.2. *There exists $C > 0$ depending on Γ_D, but independent of the mesh-boundary intersection, such that for every $K \in \mathcal{M}$*

$$\|v\|^2_{L^2(\Gamma_K)} \leq C \left(\left\| \mathsf{h}^{-\frac{1}{2}} v \right\|^2_{L^2(K)} + \left\| \mathsf{h}^{\frac{1}{2}} \nabla v \right\|^2_{L^2(K)} \right) \qquad \forall\, v \in H^1(K).$$

Proof. It follows straightforward from Lemma 3 in [21]. ∎

Hence we can apply the previous result to obtain

$$\left\| \frac{\partial v_h}{\partial n} \right\|^2_{L^2(\Gamma_K)} \leq C \left(\left\| \mathsf{h}^{-\frac{1}{2}} \nabla v_h \right\|^2_{L^2(K)} + \left\| \mathsf{h}^{\frac{1}{2}} D^2 v_h \right\|^2_{L^2(K)} \right) \qquad \forall\, v_h \in \widetilde{V}_h.$$

By a standard inverse inequality, see [3], we get

$$\left\| D^2 v_h \right\|^2_{L^2(K)} \leq C \left\| \mathsf{h}^{-1} \nabla v_h \right\|^2_{L^2(K)} \qquad \forall\, v_h \in \widetilde{V}_h,$$

where $C > 0$ depends on the shape regularity constant. Hence we can state the following result.

COROLLARY 4.3. *There exists $C > 0$ depending on Γ_D, but independent of the mesh-boundary intersection, such that for every $K \in \mathcal{M}$*

$$\left\| \frac{\partial v_h}{\partial n} \right\|_{L^2(\Gamma_K)} \leq C \left\| \mathsf{h}^{-\frac{1}{2}} \nabla v_h \right\|_{L^2(K)} \qquad \forall\, v_h \in \widetilde{V}_h.$$

5. A new stabilization technique. The goal is to present a new, parameter free stabilization technique for the problem (3.2). Our construction is inspired by the work of J. Haslinger and Y. Renard in [22].

Let us partition the elements of the Bézier mesh into two disjoint sub-families.

DEFINITION 5.1. *Fix $\theta \in (0,1]$ and let $Q \in \widehat{\mathcal{M}}$. We say that Q is a* good element *if*

$$\frac{\text{meas}_d\left(\widehat{\Omega} \cap Q\right)}{\text{meas}_d\left(Q\right)} \geq \theta_{\min}. \tag{5.1}$$

Otherwise, Q is a bad element. *Thanks to the regularity Assumption 2.4 on $\mathbf{F}$, this classification on the parametric elements induces naturally a classification on the physical elements, see Figure 4.*

We denote as $\mathcal{M}^g$ the collection of the good physical Bézier elements and as $\mathcal{M}^b$ the one of the bad physical elements. Note that $\mathcal{M} \setminus \mathcal{G}_h \subseteq \mathcal{M}^g$ and $\mathcal{M}^b \subseteq \mathcal{G}_h$.

ASSUMPTION 5.2. *Letting $K \in \mathcal{M}$ and denoting the neighbours of K as*

$$\mathcal{N}(K) := \{K' \in \mathcal{M} : K \cap K' = f, \\ \text{where } f \text{ is either a common face, edge or vertex of } K \text{ and } K'\},$$

we assume that for any $K \in \mathcal{M}^b$ there exists $K' \in \mathcal{N}(K) \cap \mathcal{M}^g$.

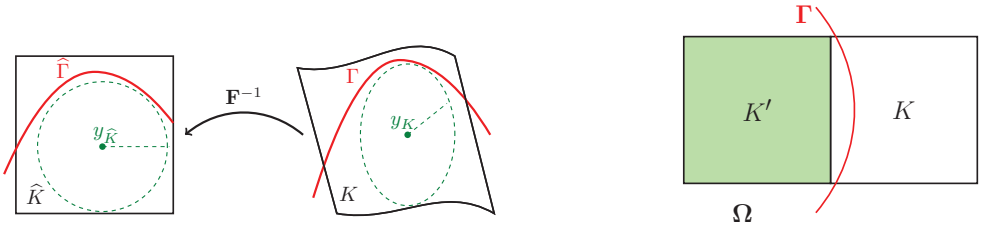

(a) K is a good element.

(b) K is a bad element and K' is a good neighbour.

Fig. 4: Illustration of good and bad elements of Definition 5.1 and Assumption 5.2.

Remark 5.3. The previous assumption holds true if the mesh is sufficiently refined. One could also relax the notion of a neighbour: $\text{dist}\,(K, K') \leq Ch$, where $C > 0$ does not depend on h.

Now let us assume that there exists an operator

$$R_h : \widetilde{V}_h \to L^2(\Gamma_D)$$

which approximates the normal derivative on Γ_D in a sense that will be specified below. We propose the following stabilized formulation of problem (3.2).

Find $u_h \in \widetilde{V}_h$ such that

$$\overline{a}_h(u_h, v_h) = \int_\Omega f v_h + \int_{\Gamma_N} g_N v_h - \int_{\Gamma_D} g_D R_h(v_h) + \beta \int_{\Gamma_D} \mathsf{h}^{-1} g_D v_h \qquad \forall\, v_h \in \widetilde{V}_h, \tag{5.2}$$

where

$$\overline{a}_h(u_h, v_h) := \int_\Omega \nabla u_h \cdot \nabla v_h - \int_{\Gamma_D} R_h(u_h) v_h - \int_{\Gamma_D} u_h R_h(v_h) + \beta \int_{\Gamma_D} \mathsf{h}^{-1} u_h v_h.$$

THEOREM 5.4. *Suppose the following* stability property *is satisfied: there exists a uniform $C > 0$ such that for every $K \in \mathcal{G}_h$*

$$\left\| \mathsf{h}^{\frac{1}{2}} R_h(v_h) \right\|_{L^2(\Gamma_K)} \leq C \left\| \nabla v_h \right\|_{L^2(\Omega \cap K')} \qquad \forall\, v_h \in \widetilde{V}_h, \tag{5.3}$$

where $K' = K$ if $K \in \mathcal{M}^g$, otherwise $K' \in \mathcal{N}(K) \cap \mathcal{M}^g$. Then problem (5.2) is well-posed in the sense that the bilinear form $\overline{a}_h(\cdot,\cdot)$ is continuous and coercive with respect to $\|\cdot\|_{1,h,\Omega}$ for a sufficiently large β.

Proof. For the continuity, let $u_h, v_h \in \widetilde{V}_h$ and estimate

$$\begin{aligned}
&|\overline{a}_h(u_h, v_h)| \leq \|\nabla u_h\|_{L^2(\Omega)} \|\nabla v_h\|_{L^2(\Omega)} + \left\| \mathsf{h}^{\frac{1}{2}} R_h(u_h) \right\|_{L^2(\Gamma_D)} \left\| \mathsf{h}^{-\frac{1}{2}} v_h \right\|_{L^2(\Gamma_D)} \\
&+ \left\| \mathsf{h}^{\frac{1}{2}} R_h(v_h) \right\|_{L^2(\Gamma_D)} \left\| \mathsf{h}^{-\frac{1}{2}} u_h \right\|_{L^2(\Gamma_D)} + \beta \left\| \mathsf{h}^{-\frac{1}{2}} g_D \right\|_{L^2(\Gamma_D)} \left\| \mathsf{h}^{-\frac{1}{2}} v_h \right\|_{L^2(\Gamma_D)} \\
&\leq \|u_h\|_{1,h,\Omega} \|v_h\|_{1,h,\Omega} + C \|\nabla u_h\|_{L^2(\Omega)} \|v_h\|_{1,h,\Omega} + C \|\nabla v_h\|_{L^2(\Omega)} \|u_h\|_{1,h,\Omega} \\
&+ \beta \|u_h\|_{1,h,\Omega} \|v_h\|_{1,h,\Omega} \leq C \|u_h\|_{1,h,\Omega} \|v_h\|_{1,h,\Omega},
\end{aligned}$$

where we employed first Cauchy-Schwarz inequality, then the definition of the norm (4.1) and the stability property (5.3).

Take $u_h \in \widetilde{V}_h$. Using Young inequality and, again, the stability property (5.3), we obtain

$$\begin{aligned}
a_h(u_h, u_h) &= \|\nabla u_h\|^2_{L^2(\Omega)} - 2 \int_{\Gamma_D} R_h(u_h) u_h + \beta \left\| \mathsf{h}^{-\frac{1}{2}} u_h \right\|^2_{L^2(\Gamma_D)} \\
&\geq \|\nabla u_h\|^2_{L^2(\Omega)} - \frac{1}{\alpha} \left\| \mathsf{h}^{\frac{1}{2}} R_h(u_h) \right\|^2_{L^2(\Gamma_D)} - \alpha \left\| \mathsf{h}^{-\frac{1}{2}} u_h \right\|^2_{L^2(\Gamma_D)} \\
&\quad + \beta \left\| \mathsf{h}^{-\frac{1}{2}} u_h \right\|^2_{L^2(\Gamma_D)} \geq \left(1 - \frac{C}{\alpha}\right) \|\nabla u_h\|^2_{L^2(\Omega)} + (\beta - \alpha) \left\| \mathsf{h}^{-\frac{1}{2}} u_h \right\|^2_{L^2(\Gamma_D)},
\end{aligned}$$

from which we deduce the coercivity, provided $C < \alpha < \beta$. ∎

Remark 5.5. In order for the solution of (5.2) to be a good approximation of u, it is clear that we will also need to quantify the error between $R_h(u_h)$ and $\frac{\partial u}{\partial n}$. This fact will be addressed in the next section.

6. Construction of the stabilization operator. The definition of the operator R_h is not unique. As already observed, we seek for a stable approximation of the normal derivative on the trimmed part of the boundary, namely on Γ_K for every $K \in \mathcal{G}_h$.

Here, for instance, we propose two different constructions of such an operator.

- a *stabilization in the parametric domain*: for each $K \in \mathcal{M}^b$ we take the (unique) polynomial extension of the pull-back of the functions of $\widetilde{V}_h$ from $Q' = \mathbf{F}^{-1}(K')$ to $Q = \mathbf{F}^{-1}(K)$, where K' is a good neighbour;
- a *stabilization in the physical domain*: for each $K \in \mathcal{M}^b$, we first take the L^2-projection of the spline functions restricted to the good neighbour K' onto the polynomial space $\mathbb{Q}_p(K')$, then we take their (unique) polynomial extension to K.

DEFINITION 6.1 (Stabilization in the parametric domain). *We define the operator R_h locally as $R_h(v_h)\big|_K := R_K(v_h)\ \forall\ K \in \mathcal{G}_h,\ \forall\ v_h \in \widetilde{V}_h$, where*

- *if $K \in \mathcal{M}^g$,*

$$R_K(v_h) := \frac{\partial v_h\big|_K}{\partial n};$$

- *if $K = \mathbf{F}(Q) \in \mathcal{M}^b$, $K' = \mathbf{F}(Q') \in \mathcal{N}(K) \cap \mathcal{M}^g$,*

$$R_K(v_h) := \frac{\partial \left(\mathcal{E}\left(\widehat{v}_h\big|_{Q'}\right) \circ \mathbf{F}^{-1}\right)}{\partial n},$$

where $\mathcal{E} : \mathbb{Q}_p(Q') \to \mathbb{Q}_p(Q' \cup Q)$ is the polynomial natural extension.

DEFINITION 6.2 (Stabilization in the physical domain). *An alternative stabilization operator can be defined by using the L^2-projection in the physical domain. We define the operator R_h locally as $R_h(v_h)\big|_K := R_K(v_h)\ \forall\ K \in \mathcal{G}_h,\ \forall\ v_h \in \widetilde{V}_h$:*

- *if $K \in \mathcal{M}^g$,*

$$R_K(v_h) := \frac{\partial v_h\big|_K}{\partial n};$$

- *if $K = \mathbf{F}(Q) \in \mathcal{M}^b$, $K' \in \mathcal{N}(K) \cap \mathcal{M}^g$,*

$$R_K(v_h) := \frac{\partial \left(\mathcal{E}\left(P(v_h\big|_{K'})\right)\right)}{\partial n},$$

where $P : L^2(K') \to \mathbb{Q}_p(K')$ is the L^2-orthogonal projection. For any $u \in L^2(K')$,

$$\int_{K'} P(u)v_h = \int_{K'} uv_h \qquad \forall\ v_h \in \mathbb{Q}_p(K')$$

and $\mathcal{E} : \mathbb{Q}_p(K') \to \mathbb{Q}_p(K' \cup K)$ is the polynomial natural extension.

Remark 6.3. Note that in the trivial case where $\mathbf{F} = \mathbf{Id}$, the L^2-projection P, restricted to $\widetilde{V}_h$, reduces to the identity operator and the two stabilizations coincide.

6.1. Properties of the stabilization in the parametric domain. We are now up to verify if our choice of R_h verifies the stability property (5.3). Its proof relies on a series of quite technical results, all reported in Appendix A.

THEOREM 6.4. *The stability property (5.3) holds for R_h defined as in Definition 6.1, i.e., there exists $C > 0$ such that for every $K \in \mathcal{G}_h$*

$$\left\| \mathsf{h}^{\frac{1}{2}} R_h(v_h) \right\|_{L^2(\Gamma_K)} \leq C \left\| \nabla v_h \right\|_{L^2(\Omega \cap K')} \qquad \forall\ v_h \in \widetilde{V}_h,$$

where $K' = K$ if $K \in \mathcal{M}^g$, otherwise $K' \in \mathcal{N}(K) \cap \mathcal{M}^g$.

Proof. Fixed $K \in \mathcal{G}_h$, it is enough to prove

$$\left\| \mathsf{h}^{\frac{1}{2}} \widetilde{v}_h \right\|_{L^2(\Gamma_K)} \leq C \left\| v_h \right\|_{L^2(\Omega \cap K')},$$

for $v_h \in \widetilde{V}_h$ such that $\widetilde{v}_h\big|_K := \mathcal{E}\left(\widehat{v}_h\big|_{Q'}\right) \circ \mathbf{F}^{-1}$, where $\mathcal{E} : \mathbb{P}_p(Q') \to \mathbb{P}_p(Q' \cup Q)$ and $K = \mathbf{F}(Q)$, $K' = \mathbf{F}(Q') \in \mathcal{N}(K) \cap \mathcal{M}^g$.

We can restrict ourselves to the bad elements. Let $K \in \mathcal{M}^b$ with good neighbour K'. It holds that

$$\begin{aligned}\|\widetilde{v}_h\|^2_{L^2(\Gamma_K)} &= \int_{\Gamma_K} |\widetilde{v}_h|^2 \,\mathrm{d}S = \int_{\mathbf{F}^{-1}(\Gamma_K)} |\widehat{v}_h|^2 \left|\det\left(D\mathbf{F}\right)\right| \left\|D\mathbf{F}^{-1}\widehat{\mathbf{n}}\right\| \mathrm{d}\widehat{S} \\ &\leq C \int_{\mathbf{F}^{-1}(\Gamma_K)} |\widehat{v}_h|^2 \,\mathrm{d}\widehat{S} = C \|\widehat{v}_h\|^2_{L^2(\widehat{\Gamma}_D \cap Q)}\,,\end{aligned} \tag{6.1}$$

where we have used $\mathbf{F}^{-1}(\Gamma_K) = \mathbf{F}^{-1}(\Gamma_D) \cap \mathbf{F}^{-1}(K) = \widehat{\Gamma}_D \cap Q$, because $\mathbf{F}$ preserves boundaries (as homeomorphisms do).

We then have

$$\begin{aligned}\|\widehat{v}_h\|_{L^2(\widehat{\Gamma}_D \cap Q)} &\leq \mathrm{meas}_{d-1}\left(\widehat{\Gamma}_D \cap Q\right)^{\frac{1}{2}} \|\widehat{v}_h\|_{L^\infty(\widehat{\Gamma}_D \cap Q)} \\ &\leq \mathrm{meas}_{d-1}\left(\widehat{\Gamma}_D \cap Q\right)^{\frac{1}{2}} \|\widehat{v}_h\|_{L^\infty(Q)}\,.\end{aligned}$$

In the first inequality we have used Hölder inequality, while the second one is straightforward.

Now, we continue employing, respectively, Lemma A.1 and Assumption 3.1:

$$\|\widehat{v}_h\|^2_{L^2(\widehat{\Gamma}_D \cap Q)} \leq C\,\mathrm{meas}_{d-1}\left(\widehat{\Gamma}_D \cap Q\right)^{\frac{1}{2}} \|\widehat{v}_h\|_{L^\infty(Q')} \leq C h_{\max}^{\frac{d-1}{2}} \|\widehat{v}_h\|_{L^\infty(Q')}\,.$$

At this point, notice that we can use Lemma A.2 because $\frac{\mathrm{meas}_d\left(\Omega \cap K'\right)}{\mathrm{meas}_d(K')} \geq \theta_{\min}$ implies $\frac{\mathrm{meas}_d\left(\widehat{\Omega} \cap Q'\right)}{\mathrm{meas}_d(Q')} \geq C\theta_{\min}$, where C depends just on $\mathbf{F}$, thanks to Assumption 2.4.

Let us continue with the inequalities:

$$\|\widehat{v}_h\|_{L^2(\widehat{\Gamma}_D \cap Q)} \leq C h_{\min}^{-\frac{1}{2}} \|\widehat{v}_h\|_{L^2(\widehat{\Omega} \cap Q')} \leq C h_{\min}^{-\frac{1}{2}} \|v_h\|_{L^2(\Omega \cap K')}\,. \tag{6.2}$$

Gathering together (6.1) and (6.2), we conclude the proof. ∎

In what follows, we analyse the approximation properties of the operator R_h, and provide estimates that will be used then in Section 7 to deduce a complete error estimate.

Proposition 6.5. *Let $0 \leq k \leq p$ and*

$$\Pi_0 : H^{k+1}(\Omega_0) \to \widetilde{V}_h$$

be a spline quasi-interpolation operator ([9]).

There exists $C > 0$ such that for every $K \in \mathcal{G}_h$

- *if $0 \leq k < p - \frac{1}{2}$, for every $v \in H^{k+1}(\Omega_0)$*

$$\left\| \mathsf{h}^{\frac{1}{2}} \left(R_h\left(\Pi_0(v)\right) - \frac{\partial v}{\partial n} \right) \right\|_{L^2(\Gamma_K)} \leq C h_{\max}^k \|v\|_{H^{k+1}\left(\widetilde{K} \cup \widetilde{K}'\right)}\,,$$

  where $K' = K$ if $K \in \mathcal{M}^g$, otherwise $K' \in \mathcal{N}(K) \cap \mathcal{M}^g$;
- *if $p - \frac{1}{2} \leq k \leq p$ and each internal knot line is not repeated, for every $v \in H^{k+1}(\Omega_0)$, for all $\varepsilon > 0$,*

$$\left\| \mathsf{h}^{\frac{1}{2}} \left(R_h\left(\Pi_0(v)\right) - \frac{\partial v}{\partial n} \right) \right\|_{L^2(\Gamma_K)} \leq C h_{\max}^{p-\frac{1}{2}-\varepsilon} \|v\|_{H^{k+1}\left(\widetilde{K} \cup \widetilde{K}'\right)}\,,$$

where $K' = K$ if $K \in \mathcal{M}^g$, otherwise $K' \in \mathcal{N}(K) \cap \mathcal{M}^g$.

Proof. First of all, let $v \in H^{k+1}(\Omega_0)$, with $0 \leq k \leq p$.

We take $K \in \mathcal{G}_h$. Let us distinguish two cases: K is a good element and K is a bad element.

If $K \in \mathcal{M}^g$. We use Lemma 4.2 and standard approximation results:

$$\begin{aligned}
&\left\| \mathsf{h}^{\frac{1}{2}} \left(R_h\left(\Pi_0(v)\right) - \frac{\partial v}{\partial n} \right) \right\|_{L^2(\Gamma_K)} = \left\| \mathsf{h}^{\frac{1}{2}} \left(\frac{\partial \Pi_0(v)}{\partial n} - \frac{\partial v}{\partial n} \right) \right\|_{L^2(\Gamma_K)} \\
\leq & C \Big(\left\| \nabla \Pi_0(v) - \nabla v \right\|_{L^2(K)} + \left\| \mathsf{h}(\nabla \Pi_0(v) - \nabla v) \right\|_{H^1(K)} \Big) \\
\leq & C \left(\left\| \mathsf{h}^k v \right\|^2_{H^{k+1}(\tilde{K})} + \left\| \mathsf{h}^k v \right\|^2_{H^{k+1}(\tilde{K})} \right) \leq 2C h^k_{\max} \left\| v \right\|^2_{H^{k+1}(\tilde{K})}.
\end{aligned}$$

If $K = \mathbf{F}(Q) \in \mathcal{M}^b$ and $K' = \mathbf{F}(Q') \in \mathcal{N}(K) \cap \mathcal{M}^g$ be its good neighbour. We easily obtain

(6.3)
$$\begin{aligned}
&\left\| \mathsf{h}^{\frac{1}{2}} \left(R_h\left(\Pi_0(v)\right) - \frac{\partial v}{\partial n} \right) \right\|_{L^2(\Gamma_K)} \leq C \left\| \mathsf{h}^{\frac{1}{2}} \left(\frac{\partial}{\partial n} \mathcal{E}\left(\Pi_0\left(v\right) \circ \mathbf{F}\big|_{Q'} \right) - \frac{\partial \widehat{v}}{\partial n} \right) \right\|_{L^2(\widehat{\Gamma}_D \cap Q)} \\
\leq & C \Big(\left\| \mathsf{h}^{\frac{1}{2}} \frac{\partial}{\partial n} \left(\mathcal{E}\left(\Pi_0\left(v\right) \circ \mathbf{F}\big|_{Q'} \right) - \Pi_0\left(v\right) \circ \mathbf{F} \right) \right\|_{L^2(\widehat{\Gamma}_D \cap Q)} \\
& + \left\| \mathsf{h}^{\frac{1}{2}} \frac{\partial}{\partial n} \left(\Pi_0\left(v\right) \circ \mathbf{F} - \widehat{v} \right) \right\|_{L^2(\widehat{\Gamma}_D \cap Q)} \Big).
\end{aligned}$$

The second term converges as expected because of the properties of spline quasi-interpolants [9]. We focus on the first one.

Let $\widehat{q} = q \circ \mathbf{F} \in \mathbb{Q}_p(\mathbb{R}^d)$ be a global polynomial. Note that, trivially, $\mathcal{E}(\widehat{q}\big|_{Q'}) = \widehat{q}\big|_{Q'}$. By triangular inequality:

$$\begin{aligned}
&\left\| \mathsf{h}^{\frac{1}{2}} \frac{\partial}{\partial n} \left(\mathcal{E}\left(\Pi_0\left(v\right) \circ \mathbf{F}\big|_{Q} \right) - \Pi_0\left(v\right) \circ \mathbf{F} \right) \right\|_{L^2(\widehat{\Gamma}_D \cap Q)} \\
\leq & \left\| \mathsf{h}^{\frac{1}{2}} \frac{\partial}{\partial n} \mathcal{E}\left(\Pi_0\left(v\right) \circ \mathbf{F}\big|_{Q} - \widehat{q} \right) \right\|_{L^2(\widehat{\Gamma}_D \cap Q)} + \left\| \mathsf{h}^{\frac{1}{2}} \frac{\partial}{\partial n} \left(\widehat{q} - \Pi_0\left(v\right) \circ \mathbf{F} \right) \right\|_{L^2(\widehat{\Gamma}_D \cap Q)}.
\end{aligned} \tag{6.4}$$

Using Corollary 4.3, we can bound the last term of (6.4) as follows:

$$\left\| \mathsf{h}^{\frac{1}{2}} \frac{\partial}{\partial n} \left(\Pi_0\left(v\right) \circ \mathbf{F} - \widehat{q} \right) \right\|_{L^2(\widehat{\Gamma}_D \cap Q))} \leq C \left\| \left(\Pi_0\left(v\right) \circ \mathbf{F} - \widehat{q} \right) \right\|_{H^1(Q)}. \tag{6.5}$$

The first term of (6.4) can be bounded using the stability property of R_h, given in Theorem 6.4:

$$\left\| \mathsf{h}^{\frac{1}{2}} \frac{\partial}{\partial n} \mathcal{E}\left(\Pi_0\left(v\right) \circ \mathbf{F}\big|_{Q} - \widehat{q} \right) \right\|_{L^2(\widehat{\Gamma}_D \cap Q)} \leq C \left\| \nabla \left(\Pi_0\left(v\right) \circ \mathbf{F} - \widehat{q} \right) \right\|_{L^2(\widehat{\Omega} \cap Q')}. \tag{6.6}$$

Thus, combining (6.3), (6.4), (6.5) and (6.6), we obtain

$$\begin{aligned}
&\left\| \mathsf{h}^{\frac{1}{2}} \frac{\partial}{\partial n} \left(\mathcal{E}\left(\Pi_0\left(v\right) \circ \mathbf{F}\big|_{Q} \right) - \Pi_0\left(v\right) \circ \mathbf{F} \right) \right\|_{L^2(\widehat{\Gamma}_D \cap Q)} \\
\leq & C \left\| \left(\Pi_0\left(v\right) \circ \mathbf{F}\big|_{Q} - \widehat{q} \right) \right\|_{H^1(Q \cup Q')} \\
\leq & C \Big(\left\| \left(\Pi_0\left(v\right) - v \right) \circ \mathbf{F} \right\|_{H^1(Q \cup Q')} + \left\| \left(v \circ \mathbf{F} - \widehat{q} \right) \right\|_{H^1(Q \cup Q')} \Big).
\end{aligned} \tag{6.7}$$

Again, the first term converges as expected by standard approximation results. Concerning the other term, there are some issues, related to the regularity of the parametrization. In fact, we have $v \in H^{k+1}(\Omega_0)$, but, in general, $v \circ \mathbf{F}\big|_{Q\cup Q'} \notin H^{k+1}(Q \cup Q')$, since it is bent by $\mathbf{F}$, a spline of degree p and regularity $p-1$ (under the assumption that internal knot lines are not repeated). It holds, indeed, that $v \circ \mathbf{F}\big|_{Q\cup Q'} \in H^{r+1}(Q \cup Q')$, where $r+1 := \min\{k+1, p+\frac{1}{2}-\varepsilon\}$, hence $0 \le r \le k$ and $0 \le r \le p-\frac{1}{2}-\varepsilon$. So, the following inequality holds:

$$\|v \circ \mathbf{F} - \widehat{q}\|_{H^1(Q\cup Q')} \le C h_{\max}^r \|v \circ \mathbf{F}\|_{H^{r+1}(\widetilde{Q}\cup\widetilde{Q}')},$$

where $0 \le r \le k$ and $0 \le r \le p-\frac{1}{2}-\varepsilon$, for any $\varepsilon > 0$. Hence, pushing forward to the physical domain

$$\|v - q\|_{H^1(K\cup K')} \le C h_{\max}^r \|v\|_{H^{r+1}(\widetilde{K}\cup\widetilde{K}')}. \tag{6.8}$$

Hence, from (6.7) and (6.8), we deduce

$$\begin{aligned} &\left\| \mathsf{h}^{\frac{1}{2}} \left(R_h\left(\Pi_0(v)\right) - \frac{\partial v}{\partial n} \right) \right\|_{L^2(\Gamma_K)} \\ \le & C\Big(h_{\max}^k \|v\|_{H^{k+1}(\widetilde{K}\cup\widetilde{K}')} + h_{\max}^r \|v\|_{H^{r+1}(\widetilde{K}\cup\widetilde{K}')} \Big). \end{aligned} \tag{6.9}$$

We want to rewrite inequality (6.9) by distinguishing two cases.

- $0 \le k < p-\frac{1}{2}$. In this case,

$$\left\| \mathsf{h}^{\frac{1}{2}} \left(R_h\left(\Pi_0(v)\right) - \frac{\partial v}{\partial n} \right) \right\|_{L^2(\Gamma_K)} \le C h_{\max}^k \|v\|_{H^{k+1}(\widetilde{K}\cup\widetilde{K}')}, \tag{6.10}$$

  for $0 \le r \le k$.
- If $p-\frac{1}{2} \le k \le p$, then

$$\left\| \mathsf{h}^{\frac{1}{2}} \left(R_h\left(\Pi_0(v)\right) - \frac{\partial v}{\partial n} \right) \right\|_{L^2(\Gamma_K)} \le C h_{\max}^{p-\frac{1}{2}-\varepsilon} \|v\|_{H^{k+1}(\widetilde{K}\cup\widetilde{K}')}, \tag{6.11}$$

  for any $\varepsilon > 0$.

Hence, the thesis is proven. ∎

Remark 6.6. Note that if $0 \le k < p-\frac{1}{2}$, the estimate is optimal. In the case $p-\frac{1}{2} \le k \le p$ the estimate is sub-optimal, instead. Moreover, if the knot line between K and K' has multiplicity higher than one, then the sub-optimality is even worse. We will see an example of this sub-optimal behaviour in Section 8.

6.2. Properties of the stabilization in the physical domain.

THEOREM 6.7. *The stability property* (5.3) *holds for* R_h *defined as in Definition 6.2, i.e., there exists* $C > 0$ *such that for every* $K \in \mathcal{G}_h$

$$\left\| \mathsf{h}^{\frac{1}{2}} R_h(v_h) \right\|_{L^2(\Gamma_K)} \le C \|\nabla v_h\|_{L^2(\Omega\cap K')} \qquad \forall\, v_h \in \widetilde{V}_h,$$

where $K' = K$ *if* $K \in \mathcal{M}^g$, *otherwise* $K' \in \mathcal{N}(K) \cap \mathcal{M}^g$.

Proof. Let us start applying Hölder inequality and Lemma A.1

$$\begin{aligned}\|R_h(v_h)\|_{L^2(\Gamma_K)} =& \left\| \frac{\partial}{\partial n} \mathcal{E}\left(P(v_h|_{K'})\right)\right\|_{L^2(\Gamma_K)} \\ \leq& \sqrt{\mathrm{meas}_{d-1}(\Gamma_K)} \left\| \frac{\partial}{\partial n} \mathcal{E}\left(P(v_h|_{K'})\right)\right\|_{L^\infty(\Gamma_K)} \\ \leq& \sqrt{\mathrm{meas}_{d-1}(\Gamma_K)} \left\|\nabla \mathcal{E}\left(P(v_h|_{K'})\right)\right\|_{L^\infty(K)} \\ \leq& C\sqrt{\mathrm{meas}_{d-1}(\Gamma_K)} \left\|\nabla P(v_h|_{K'})\right\|_{L^\infty(K')}.\end{aligned}$$

We finish with Lemma A.2, Assumption 3.1 and the stability of the L^2-orthogonal projection P, see for instance [6],

$$\begin{aligned}\left\|\mathsf{h}^{\frac{1}{2}} R_h(v_h)\right\|_{L^2(\Gamma_K)} \leq& C h_{\min}^{-\frac{d}{2}} \sqrt{\mathrm{meas}_{d-1}(\Gamma_K)} \left\|\mathsf{h}^{\frac{1}{2}} \nabla P(v_h|_{K'})\right\|_{L^2(\Omega\cap K')} \\ \leq& C\|\nabla P(v_h)\|_{L^2(\Omega\cap K')} \leq C\|\nabla v_h\|_{L^2(\Omega\cap K')}.\end{aligned}$$

We conclude by summing over $K \in \mathcal{G}_h$. ∎

Proposition 6.8. *Let $0 \leq k \leq p$ and*

$$\Pi_0 : H^{k+1}(\Omega_0) \to \widetilde{V}_h$$

be a spline quasi-interpolation operator [9]. There exists $C > 0$ such that for every $K \in \mathcal{G}_h$

$$\left\|\mathsf{h}^{\frac{1}{2}} \left(R_h\left(\Pi_0(v)\right) - \frac{\partial v}{\partial n}\right)\right\|_{L^2(\Gamma_K)} \leq C h_{\max}^k \|v\|_{H^{k+1}\left(\widetilde{K}\cup\widetilde{K}'\right)} \qquad \forall\, v \in H^{k+1}(\Omega_0),$$

where $K' = K$ if $K \in \mathcal{M}^g$, otherwise $K' \in \mathcal{N}(K) \cap \mathcal{M}^g$.

Proof. We can focus on the case $K \in \mathcal{M}^b$. Let $K' \in \mathcal{N}(K) \cap \mathcal{M}^g$ and $q \in \mathbb{Q}_p(K')$.

$$\begin{aligned}&\left\|\mathsf{h}^{\frac{1}{2}} \left(R_h\left(\Pi_0(v)\right) - \frac{\partial v}{\partial n}\right)\right\|_{L^2(\Gamma_K)} = \left\|\mathsf{h}^{\frac{1}{2}} \frac{\partial}{\partial n}\left(\mathcal{E}\left(P\left(\Pi_0(v)|_{K'}\right)\right) - v\right)\right\|_{L^2(\Gamma_K)} \\ \leq& \left\|\mathsf{h}^{\frac{1}{2}} \frac{\partial}{\partial n}\left(\mathcal{E}\left(P\left(\Pi_0(v)|_{K'}\right)\right) - q\right)\right\|_{L^2(\Gamma_K)} + \left\|\mathsf{h}^{\frac{1}{2}} \frac{\partial}{\partial n}(q - v)\right\|_{L^2(\Gamma_K)}.\end{aligned} \tag{6.12}$$

Let us focus on the first term. After having observed that $P(q) = q$, we apply the stability property proved in Theorem 6.7 and, again, triangular inequality

$$\begin{aligned}&\left\|\mathsf{h}^{\frac{1}{2}} \frac{\partial}{\partial n}\left(\mathcal{E}\left(P\left(\Pi_0(v)|_{K'}\right)\right) - q\right)\right\|_{L^2(\Gamma_K)} \leq C\|\nabla\left(\Pi_0(v) - q\right)\|_{L^2(\Omega\cap K')} \\ \leq& C\Big(\|\nabla(q - v)\|_{L^2(\Omega\cap K')} + \|\nabla(v - \Pi_0(v))\|_{L^2(\Omega\cap K')}\Big)\end{aligned} \tag{6.13}$$

Now, let us choose $q = P(v)$. Note that the second term of (6.12) converges as expected by the approximation properties of the L^2-projection. Plugging (6.13) into (6.12), we obtain

$$\begin{aligned}\left\|\mathsf{h}^{\frac{1}{2}} \left(R_h\left(\Pi_0(v)\right) - \frac{\partial v}{\partial n}\right)\right\|_{L^2(\Gamma_K)} \leq& C h_{\max}^k \left(\|\nabla v\|_{H^{k+1}\left(\widetilde{K}'\right)} + \|\nabla v\|_{H^{k+1}\left(\widetilde{K}\right)}\right) \\ \leq& C h_{\max}^k \|v\|_{H^{k+1}\left(\widetilde{K}\cup\widetilde{K}'\right)}.\end{aligned} \tag{6.14}$$

We conclude by summing over $K \in \mathcal{G}_h$. ∎

7. A priori error estimate. The preparatory results of Propositions 6.5 and 6.8 were needed in order to prove the following convergence theorem.

THEOREM 7.1. *Let $0 \le k \le p$, $u \in H^{k+1}(\Omega_0)$ be the solution to (3.1) and $u_h \in \widetilde{V}_h$ solution to (5.2). Then,*

$$\|u - u_h\|_{1,h,\Omega} \le C \left(h_{\max}^k \|u\|_{H^{k+1}(\Omega)} + h_{\max}^r \|u\|_{H^{r+1}(S_h)} \right), \tag{7.1}$$

where S_h is the strip of width $Ch_{\max}$, $C \ge 1$, such that $S_h \supseteq \bigcup_{K \in \mathcal{G}_h} \left(\widetilde{K} \cup \widetilde{K}' \right)$, and K' is the good neighbour of K chosen for the stabilization. Moreover

- *$0 \le r < p - \frac{1}{2}$ if we use the stabilization in the parametric domain of Definition 6.1;*
- *$0 \le r \le p$ if we use the stabilization in the physical domain of Definition 6.2.*

Proof. In view of Propositons 6.5 and 6.8, (7.1) is a simple consequence of the Bramble-Hilbert Lemma (see, for instance, [34]). From Theorems 5.4, 6.4 and 6.7 we know that $\overline{a}_h(\cdot,\cdot)$ is coercive w.r.t. $\|\cdot\|_{1,h,\Omega}$, i.e. there exists $\alpha > 0$ such that for every $u_h \in \widetilde{V}_h$

$$\alpha \sup_{\substack{w_h \in \widetilde{V}_h \\ w_h \neq 0}} \frac{\overline{a}_h(u_h, w_h)}{\|w_h\|_{1,h,\Omega}} \ge \|u_h\|_{1,h,\Omega} . \tag{7.2}$$

Let $v_h \in \widetilde{V}_h$. Using the triangular inequality and coercivity, we get:

$$\begin{aligned} \|u - u_h\|_{1,h,\Omega} &\le \|u - v_h\|_{1,h,\Omega} + \|v_h - u_h\|_{1,h,\Omega} \\ &\le \|u - v_h\|_{1,h,\Omega} + \alpha \sup_{\substack{w_h \in V_h \\ w_h \neq 0}} \frac{\overline{a}_h(v_h - u_h, w_h)}{\|w_h\|_{1,h,\Omega}} . \end{aligned} \tag{7.3}$$

Then, recalling that u solves (3.1) and u_h solves (5.2), and properly rearranging the terms, we get

$$\begin{aligned} \overline{a}_h(v_h - u_h, w_h) =& \overline{a}_h(v_h, w_h) - \overline{a}_h(u_h, w_h) \\ =& \underbrace{\int_\Omega \nabla(v_h - u) \cdot \nabla w_h}_{I} - \underbrace{\int_{\Gamma_D} (R_h(v_h) - \frac{\partial u}{\partial n}) w_h}_{II} \\ &+ \underbrace{\int_{\Gamma_D} (u - v_h) R_h(w_h)}_{III} + \underbrace{\beta \int_{\Gamma_D} \mathsf{h}^{-1} (v_h - u) w_h}_{IV} . \end{aligned}$$

Let us now estimate the four terms separately. We will leave II for last since its analysis depends on the choice of the stabilization. Clearly

$$I + IV \le C \|u - v_h\|_{1,h,\Omega} \|w_h\|_{1,h,\Omega} . \tag{7.4}$$

Using the stability property (5.3) and taking $K' \in \mathcal{N}(K) \cap \mathcal{M}^g$ (if K itself is a good element, then take $K' = K$), we get:

$$\begin{aligned} III^2 &\le \left\| \mathsf{h}^{-\frac{1}{2}} (u - v_h) \right\|^2_{L^2(\Gamma_D)} \sum_{K \in \mathcal{G}_h} \left\| \mathsf{h}^{\frac{1}{2}} R_h(w_h) \right\|^2_{L^2(\Gamma_K)} \\ &\le \|u - v_h\|^2_{1,h,\Omega} C \sum_{K \in \mathcal{G}_h} \|\nabla w_h\|^2_{L^2(K' \cap \Omega)} \le C \|u - v_h\|^2_{1,h,\Omega} \|w_h\|^2_{1,h,\Omega} . \end{aligned} \tag{7.5}$$

Let us estimate the term II:

$$\begin{aligned} II &\leq \left\| \mathsf{h}^{\frac{1}{2}} \left(R_h(v_h) - \frac{\partial u}{\partial n} \right) \right\|_{L^2(\Gamma_D)} \left\| \mathsf{h}^{-\frac{1}{2}} w_h \right\|_{L^2(\Gamma_D)} \\ &\leq \left\| \mathsf{h}^{\frac{1}{2}} \left(R_h(v_h) - \frac{\partial u}{\partial n} \right) \right\|_{L^2(\Gamma_D)} \|w_h\|_{1,h,\Omega} . \end{aligned}$$

Now, we choose $v_h = \Pi_0(u)$ and distinguish two cases corresponding to the choice of the stabilization.

- If we use the stabilization in the parametric domain of Definition 6.1, hence apply Proposition 6.5, we get

$$\begin{aligned} &\sum_{K \in \mathcal{G}_h} \left\| \mathsf{h}^{\frac{1}{2}} \left(R_h \left(\Pi_0 \left(u \right) \right) - \frac{\partial u}{\partial n} \right) \right\|_{L^2(\Gamma_K)} \|w_h\|_{1,h,\Omega} \\ &\qquad \leq \sum_{K \in \mathcal{G}_h} C \left(h_{\max}^k \|u\|_{H^{k+1}\left(\widetilde{K} \cup \widetilde{K}'\right)} + h_{\max}^r \|u\|_{H^{k+1}\left(\widetilde{K} \cup \widetilde{K}'\right)} \right) \|w_h\|_{1,h,\Omega} , \end{aligned}$$

  where $0 \leq r < p - \frac{1}{2}$.
- Employing the stabilization in the physical domain of Definition 6.2, hence apply Proposition 6.8, we obtain

$$\begin{aligned} &\sum_{K \in \mathcal{G}_h} \left\| \mathsf{h}^{\frac{1}{2}} \left(R_h \left(\Pi_0 \left(u \right) \right) - \frac{\partial u}{\partial n} \right) \right\|_{L^2(\Gamma_K)} \|w_h\|_{1,h,\Omega} \\ &\qquad \leq \sum_{K \in \mathcal{G}_h} C h_{\max}^k \|u\|_{H^{k+1}\left(\widetilde{K} \cup \widetilde{K}'\right)} \|w_h\|_{1,h,\Omega} . \end{aligned}$$

Therefore, we have that

$$II \leq C \left(h_{\max}^k \|u\|_{H^{k+1}(\Omega)} + h_{\max}^r \|u\|_{H^{k+1}(S_h)} \right) \|w_h\|_{1,h,\Omega} ,$$

where S_h is the strip of width $Ch_{\max}$, $C \geq 1$, such that $S_h \supseteq \bigcup_{K \in \mathcal{G}_h} \left(\widetilde{K} \cup \widetilde{K}' \right)$, and K', as usual, is the good neighbour of K chosen for the stabilization and

- $0 \leq r < p - \frac{1}{2}$ if we use the stabilization in the parametric domain, hence apply Proposition 6.5;
- $0 \leq r \leq p$ if we go for the one in the physical domain and use Proposition 6.8.

As a consequence, we have that

$$\begin{aligned} \overline{a}_h(\Pi_0(u) - u_h, w_h) \leq & \|u - \Pi_0(u)\|_{1,h,\Omega} \|w_h\|_{1,h,\Omega} \\ & + C \left(h_{\max}^k \|u\|_{H^{k+1}(\Omega)} + h_{\max}^r \|u\|_{H^{k+1}(S_h)} \right) \|w_h\|_{1,h,\Omega} \\ & + C \|u - \Pi_0(u)\|_{1,h,\Omega} \|w_h\|_{1,h,\Omega} , \end{aligned} \tag{7.6}$$

where in (7.4), (7.5) we choose again $v_h = \Pi_0(u)$.

We now combine the last inequality (7.6) with (7.2) and (7.3) to obtain

$$\begin{aligned} \|u - u_h\|_{1,h,\Omega} &\leq \|u - \Pi_0(u)\|_{1,h,\Omega} + \alpha \sup_{\substack{w_h \in \widetilde{V}_h \\ w_h \neq 0}} \frac{\overline{a}_h(\Pi_0(u) - u_h, w_h)}{\|w_h\|_{1,h,\Omega}} \\ &\leq (1 + \alpha(1 + C)) \|u - \Pi_0(u)\|_{1,h,\Omega} + \alpha C \left(h_{\max}^k \|u\|_{H^{k+1}(\Omega)} + h_{\max}^r \|u\|_{H^{k+1}(S_h)} \right). \end{aligned}$$

Finally, using approximation results of quasi-interpolants in spline spaces [9], we conclude

$$\|u - u_h\|_{1,h,\Omega} \leq C \left(h_{\max}^k \|u\|_{H^{k+1}(\Omega)} + h_{\max}^r \|u\|_{H^{r+1}(S_h)} \right),$$

where r is the same as above. ∎

As already observed in Remark 6.6, when $u \in H^{k+1}(\Omega)$ with $0 \leq k < p - \frac{1}{2}$, both stabilizations give rise to optimal a priori error estimates. When $u \in H^{k+1}(\Omega)$ with $p - \frac{1}{2} \leq k \leq p$, instead, stabilization in Definition 6.1 is sub-optimal. In this case, however, the estimate can be modified and improved using the following result.

LEMMA 7.2. *Let $u \in H^{p+\frac{3}{2}-\varepsilon}(\Omega_0)$ and S_h be defined as in Theorem 7.1. Then, there exists $C > 0$ such that*

$$\|u\|_{H^{r+1}(S_h)} \leq C h^{\frac{1}{2}-\varepsilon} \|u\|_{H^{p+\frac{3}{2}-\varepsilon}(\Omega)} \qquad \forall\, \varepsilon > 0,$$

for all $p - \frac{1}{2} \leq r \leq p$.

Proof. Using the fact that $r \leq p$, we are able to recover an integer order for the Sobolev norm and so to apply Lemma A.5 with $s = \frac{1}{2} - \varepsilon$:

$$\|u\|_{H^{r+1}(S_h)} \leq \|u\|_{H^{p+1}(S_h)} \leq C h_{\max}^{\frac{1}{2}-\varepsilon} \|u\|_{H^{p+\frac{3}{2}-\varepsilon}(\Omega)}.$$

∎

PROPOSITION 7.3. *Let $u \in H^{p+1}(\Omega_0)$ be the solution to (3.1) and $u_h \in \widetilde{V}_h$ solution to (5.2), obtained using the stabilization in the parametric domain of Definition 6.1. Then, there exists $C > 0$ such that*

$$\|u - u_h\|_{1,h,\Omega} \leq C h^{p'} \|u\|_{H^{p'+\frac{3}{2}}(\Omega)} \qquad \forall\, 0 \leq p' < p.$$

Proof. It immediately follows combining Theorem 7.1 and Lemma 7.2. ∎

Remark 7.4. At the prize of slightly higher regularity request, optimal convergence rate is to be expected also for stabilization in Definition 6.1.

8. Numerical examples.

8.1. Some details about the implementation. For accurate numerical integration, we decompose the trimmed elements into smaller quadrilateral tiles where we compute the integrals. These tiles are reparametrized as Bézier surfaces of the same degree p as the approximation space used to discretize our PDE, see [2] for a detailed explanation. We remark that this reparametrization is also used to compute the boundary integrals.

In order to compute the stabilization terms appearing in (5.2), first of all for each bad trimmed element $K = \mathbf{F}(Q)$ we choose a good neighbour $K' = \mathbf{F}(Q')$. Then we need to locally project functions living in K (or in Q) onto the space of polynomials on K' (or Q') and extend them. For the stabilization in the parametric domain, by taking as a basis the Bernstein polynomials on Q' the projection can be computed by knot insertion, while for the stabilization in the physical domain the L^2-projection is needed anyhow. We remark that in both cases the stabilization does not change the sparsity pattern of the stiffness matrix.

8.2. Validation of stability. In the first example we repeat the numerical experiment of Section 4 in order to validate the effectiveness of our stabilization technique. Since $\Omega_0 = (0,1)$ and, in particular, $\mathbf{F} = \mathbf{Id}$, we know that the two stabilizations techniques proposed in this paper are equivalent. We use the same degree and mesh size as in Section 4.

Let us solve the eigenvalue problem (4.3) with the stabilization in Definition 6.1 in the trimmed domain of Figure 2 for the same values of ε used in Section 4. The result is shown in Figure 5.

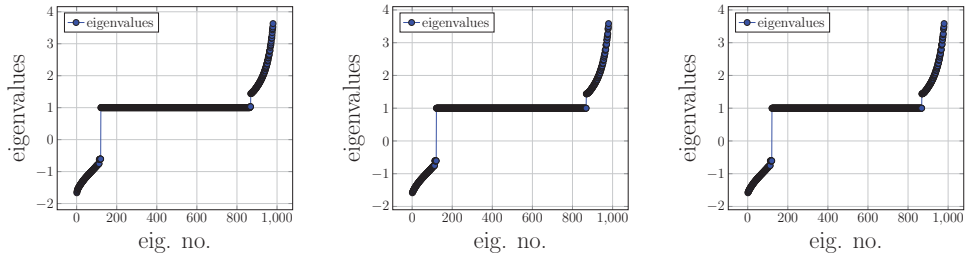

(a) Spectrum of the stabilized eigenvalue problem with $\varepsilon = 10^{-3}$.

(b) Spectrum of the stabilized eigenvalue problem with $\varepsilon = 10^{-7}$.

(c) Spectrum of the stabilized eigenvalue problem with $\varepsilon = 10^{-11}$.

Fig. 5: Generalized eigenvalues of the stabilized eigenvalue problem for different values of ε.

This time we observe that the spectrum remains bounded independently of ε, confirming our method to be robust with respect to the size of the trimming. In particular, it means that there exists $\overline{\beta} > 0$ such that for any $h > 0$, for any $\beta \geq \overline{\beta}$, $\overline{a}_h(\cdot,\cdot)$ is continuous and coercive with respect to the mesh-dependent norm $\|\cdot\|_{1,h,\Omega}$.

8.3. Validation of the a priori error estimate. We validate our method on two academic benchmarks. In the following we focus on the Poisson problem (5.2) with the difference that, while we impose Dirichlet boundary conditions weakly on the trimmed parts of the boundary, on the other parts where the mesh is fitted with the boundary we impose them in the strong sense.

Test 1. We consider the Poisson equation in the trimmed domain $\Omega = (0,1)^2 \setminus \overline{B(0,r)}$, with $r = 0.24$, see Figure 6a. We take as reference solution the smooth function $u_{ex}(x,y) = e^x \sin(xy)$. In this case the isogeometric map $\mathbf{F}$ is the identity, and as in the example of Section 8.2, the two stabilizations are equivalent. For this example the penalization parameter appearing in (5.2) is set to $\beta = 1$, and the parameter of Definition 5.1 is set to $\theta = 0.1$.

At this point, we solve the stabilized problem with different values of the degree p, and from Figure 6b we see that the theoretical results of Theorem 7.1 regarding the order of convergence are confirmed in practice.

Test 2. Let $\Omega = \Omega_0 \setminus \overline{\Omega}_1$ be defined as in Figure 7a, where $\Omega_0 = \mathbf{F}((0,1)^2)$ is a quarter of annulus constructed with biquadratic NURBS, and Ω_1 is the image of a ball in the parametric domain through the isogeometric map, namely $\Omega_1 = \mathbf{F}(B(0,r))$, with $r = 0.76$. This time we notice that the parametric and the physical domains are different and the map $\mathbf{F}$ is non-linear.

We consider as manufactured solution $u_{ex}(x,y) = e^x \sin(xy)$. We solve the PDE

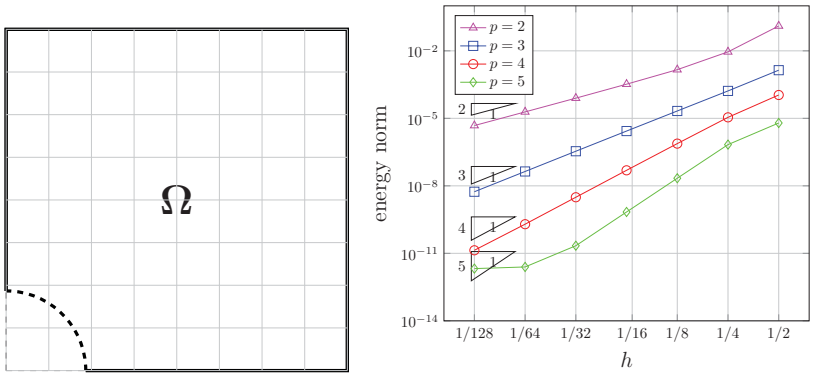

(a) Trimmed domain. (b) Convergence rates.

Fig. 6: Geometry and convergence rates for the plate with hole.

using the stabilized formulation (5.2), the stabilization in the parametric domain and the parameters $\beta = 1$ and $\theta = 0.1$. The results of convergence for different values of p, that are displayed Figure 7b, show that we obtain the optimal order of convergence.

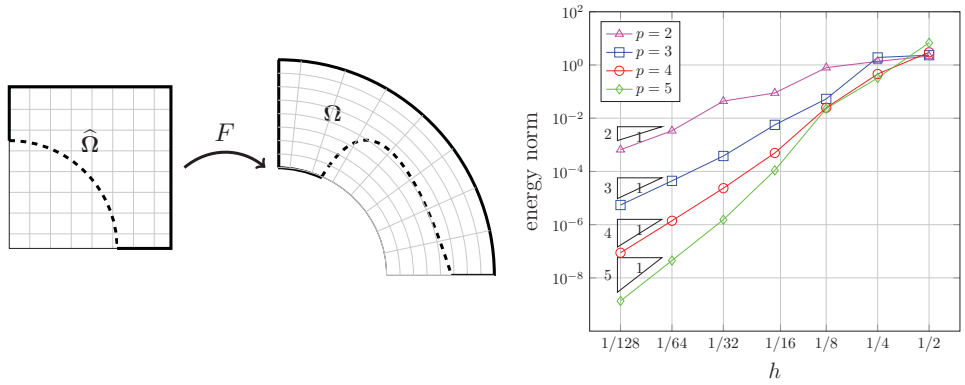

(a) Trimmed domain. (b) Convergence rates.

Fig. 7: Geometry and convergence rates for the quarter of annulus with hole.

Test 3. We now consider the Poisson problem in the L-shaped domain shown in Figure 8a, given by $\Omega = \Omega_0 \backslash \overline{\Omega}_1$, where $\Omega_0 = (-2,1)\times(-1,2)$ and $\Omega_1 = (0,1)\times(-1,0)$. The exact solution is chosen as the singular function that, in polar coordinates, reads as $u(r,\theta) = r^{\frac{2}{3}} \sin\left(\frac{2}{3}\theta\right) \in H^{\frac{5}{3}-\delta}(\Omega)$, for every $\delta > 0$. The function has a singularity at the re-entrant corner in the origin, and the domain is chosen in such a way that the corner is always located in the interior of an element. We employ the formulation (5.2) together with the stabilization operator in Definition 6.1, noting that since the parametrization is a simple scaling, both stabilizations are equivalent. This time we set the parameters $\theta = 1$ and, due to the presence of the singularity, $\beta = (p+1)\cdot 10$. The numerical results of Figure 8b agree with the theory as the method converges with

order $\frac{2}{3}$, and the sub-optimal behaviour is due to the low regularity of the reference solution.

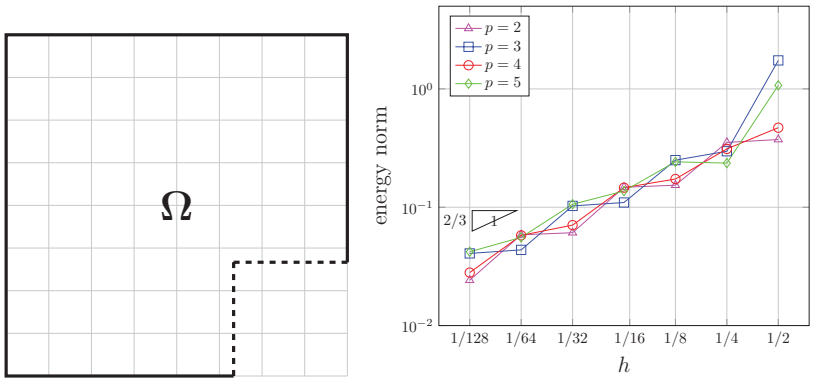

(a) Trimmed domain.

(b) Convergence rates.

Fig. 8: Geometry description and convergence rates for the L-shaped domain.

Test 4. The goal of this test is to show that in some particular situations the stabilization in the physical domain is more effective than the one in the parametric domain, as we already mentioned in Remark 6.6. Let us consider again as the domain Ω_0 the quarter of annulus, this time parametrized with a different map $\mathbf{F}$: starting from the standard biquadratic NURBS parametrization, we perform knot insertion adding the knot $\xi = 0.75$, with multiplicity 2, in the direction corresponding to the angular coordinate, that corresponds to the thick black line in Figure 9a. In order to get a geometry of class C^0, we set the second coordinate of one control point, highlighted with a big blue square in Figure 9b, equal to 0.5 in homogeneous coordinates.

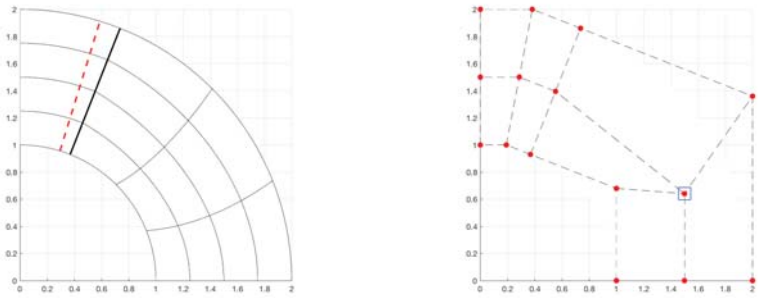

(a) Trimming line in red and dashed, C^0 knot line in thick black.

(b) Control points.

Fig. 9: Lower inter-regularity parametrization of the quarter of annulus.

Note that the new parametrization is only of class C^0 in correspondence of the knot line given by $\mathbf{F}(\{(x, y) : x \in (0, 1), y = 0.75\})$. To ensure that this

knot line is located between K and K', we define the trimmed domain as $\Omega = \mathbf{F}((0,1)\times(0,0.75+\varepsilon))$, with $\varepsilon = 10^{-8}$. Here we set $\theta = 1$ and, because of the lower regularity of the parametrization, $\beta = (p+1)\cdot 25$. We know from Remark 6.6 that the convergence rate deriving from the stabilization in Definition 6.1 will suffer of sub-optimality. In particular, from Figure 10a, we see that the error with the stabilization in the parametric domain is converging just as $h^{\frac{1}{2}}$ for any degree p, while in Figure 10b we observe that the desired convergence rates are reached when using the stabilization in the physical domain.

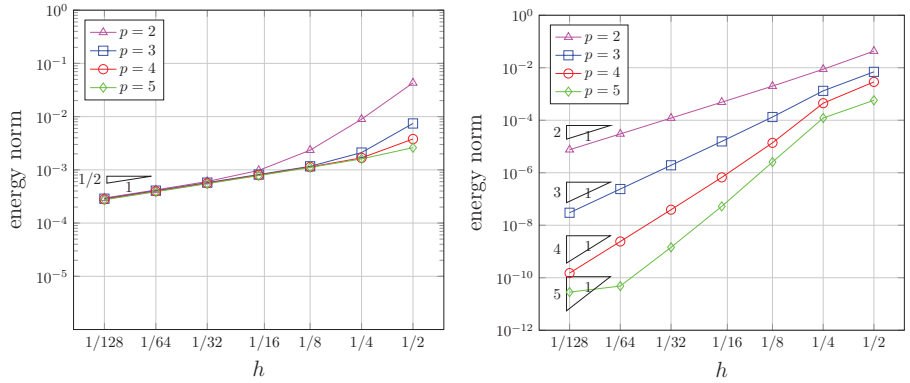

(a) Stabilization in Definition 6.1.

(b) Stabilization in Definition 6.2.

Fig. 10: Comparison of the two stabilizations in the case of an isogeometric map $\mathbf{F}$ with lower regularity.

8.4. Conditioning. Even if an exhaustive discussion about the conditioning of the stiffness matrix in trimmed geometries is beyond the scope of this work (for a more detailed discussion on the topic see, for instance, [17]), we would like to present some numerical experiments for the sake of completeness. We focus again on the formulation (5.2) of the Poisson problem.

Test 1. Let us solve the Poisson problem in two different geometries: the plate with a hole and the quarter of annulus with a hole, that we have studied above. In both cases we employ B-splines of degree $p = 3$, we impose Dirichlet boundary conditions weakly on the trimmed boundaries and strongly on the fitted ones.

In Figures 11a, 11b we show that our stabilization coupled with a simple diagonal scaling, which can be interpreted as a left-right Jacobi preconditioner, is able to solve the conditioning issue. The stabilization used is the one in the parametric domain with $\beta = 1$ and $\theta = 0.1$.

Note, however, that in the case of splines the problem does not seem to be fully understood and it is not clear if a simply rescaling suffices in general. We refer again to [17] for a more comprehensive study about conditioning in trimming.

Test 2. Finally, let $\Omega_0 = (0,1)^2$ and as trimmed domain $\Omega = (0,1)\times(0,\frac{3}{4}+\varepsilon)$, $\varepsilon > 0$, as in the test of Section 4 (see Figure 2), and we notice again that the two stabilizations are equivalent. Let us consider the stiffness matrix arising from the left hand side of problem (5.2) with Neumann boundary conditions everywhere except on the trimmed boundary, where Dirichlet boundary conditions are weakly imposed. We take B-splines of degree $p = 3$ and as mesh-size $h = \frac{1}{32}$, and we set the penalization

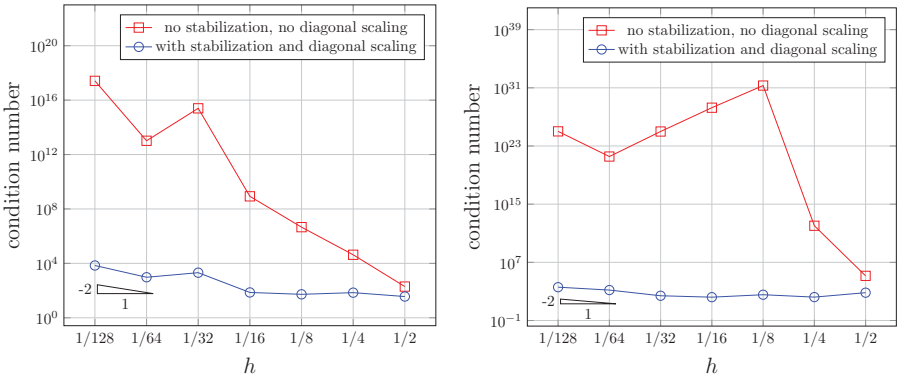

(a) Plate with a hole. (b) Quarter of annulus with a hole.

Fig. 11: Condition number versus h in two different trimmed domains.

parameter $\beta = 1$. After a simple diagonal rescaling as preconditioner, we compare the condition number of the stiffness matrix, as a function of ε, obtained for the non-stabilized ($\theta = 0$) and the stabilized ($\theta = 1$) formulations. Note that as the ratio in Definition 5.1 is the same for all cut elements, it is sufficient to consider only these two values of θ. The results in Figure 12a show the diagonal rescaling is acting as a robust preconditioner with respect to the size of the trimming. Then, we perform uniform dyadic refinement and we plot the condition number as a function of the mesh-size h, obtaining the plots in Figures 12b and 12c. The numerical results suggest a better behaviour of the condition number when a stabilized formulation is employed to solve the problem.

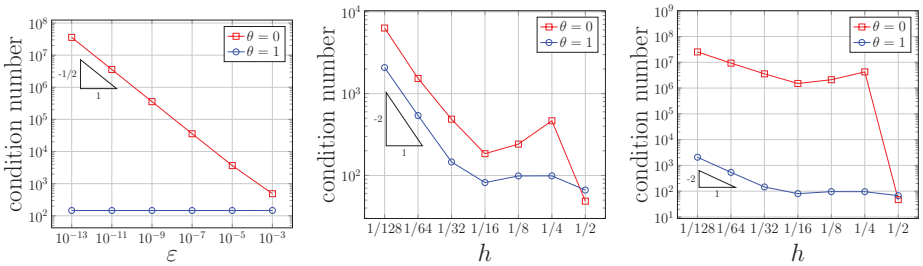

(a) Condition number vs ε. (b) Condition number vs h, with $\varepsilon = 10^{-3}$. (c) Condition number vs h, with $\varepsilon = 10^{-11}$.

Fig. 12: Condition number study in the domain of Figure 2.

Appendix A. Auxiliary theoretical results.

LEMMA A.1. *Let $Q, Q' \in \widehat{\mathcal{M}}$ be such that they either share a vertex or an edge or a face. There exists $C > 0$ such that*

$$\|p\|_{L^\infty(Q)} \leq C \, \|p\|_{L^\infty(Q')} \qquad \forall \; p \in \mathbb{Q}_k(\mathbb{R}^d),$$

where C depends on k and on the shape regularity of the mesh.

Proof. The proof easily follows by a scaling argument. ∎

The next one says that the L^2 norm on the cut portion of an element Q controls the L^∞ (and hence any other) norm on the whole element with an equivalence constant depending on the relative measure of the cut portion.

LEMMA A.2. *Let $\theta \in (0,1]$. There exists $C > 0$ such that for every $Q \in \widehat{\mathcal{M}}$ and every $S \subset Q$ measurable such that* $\mathrm{meas}_d(S) \geq \theta\, \mathrm{meas}_d(Q)$*, we have*

$$\|p\|_{L^\infty(Q)} \leq C h_{\min}^{-\frac{d}{2}} \|p\|_{L^2(S)} \qquad \forall\, p \in \mathbb{Q}_k(\mathbb{R}^d),$$

where C depends only on θ, k and the mesh regularity.

Proof. See Proposition 1 in [20]. ∎

Let us state, without proving it, a classical result by Hardy.

LEMMA A.3 (Hardy's inequality, [8]). *Let $\Omega \subset \mathbb{R}^d$ be a bounded open set of class C^1. Then there is a constant $C > 0$ such that*

$$\left\| \frac{u}{d} \right\|_{L^2(\Omega)} \leq C \|\nabla u\|_{L^2(\Omega)} \qquad \forall\, u \in H_0^1(\Omega), \tag{A.1}$$

where $d(x) := \mathrm{dist}(x, \Gamma)$.

Remark A.4. Viceversa, it is possible to characterize functions in $H_0^1(\Omega)$ as functions in $H^1(\Omega)$ such that $\frac{u}{d} \in L^2(\Omega)$ ([8]).

LEMMA A.5. *Let $\Omega_1 \subset \Omega$ with boundary Γ_1 such that $\Omega_1 = \{x \in \Omega : \mathrm{dist}(x, \Gamma) \geq C h_{\max}\}$, where $C \geq 1$ fixed and $\mathrm{dist}(\Gamma, \Gamma_1) \leq C h_{\max}$. It holds that*

$$\|v\|_{L^2(\Omega \setminus \overline{\Omega}_1)} \leq C h_{\max}^s \|v\|_{H_i^s(\Omega)} \qquad \forall\, v \in H_i^s(\Omega),$$

where the interpolation space $H_i^s(\Omega)$ or $\left(H_0^1(\Omega), L^2(\Omega)\right)_{s,2}$ is isomorphic to $H^s(\Omega)$ for $0 \leq s < \frac{1}{2}$, to $H_{00}^{\frac{1}{2}}(\Omega)$ for $s = \frac{1}{2}$ and to $H_0^s(\Omega)$ for $\frac{1}{2} < s \leq 1$ (see [41]).

Proof. We prove the following (like in [27]):

$$\|v\|_{L^2(\Omega \setminus \Omega_1)} \leq C h_{\max} \|\nabla v\|_{L^2(\Omega)} \qquad \forall\, v \in H_{0,\Gamma}^1(\Omega). \tag{A.2}$$

Let

$$d(x) := \mathrm{dist}(x, \Gamma) \qquad \forall\, x \in \Omega \setminus \overline{\Omega}_1.$$

By assumption $d(x) \leq C h_{\max}$, hence $1 \leq \frac{C h_{\max}^2}{|d(x)|^2}$, for every $x \in \Omega \setminus \overline{\Omega}_1$.

$$\int_{\Omega \setminus \overline{\Omega}_1} |v|^2 \leq C h_{\max}^2 \int_{\Omega \setminus \overline{\Omega}_1} \frac{|v|^2}{|d|^2} \leq C h_{\max}^2 \int_\Omega \frac{|v|^2}{|d|^2} \leq C h_{\max}^2 \int_\Omega |\nabla v|^2 ,$$

where we employed Hardy's inequality from Lemma A.3.

Moreover, it clearly holds that

$$\|v\|_{L^2(\Omega \setminus \overline{\Omega}_1)} \leq \|v\|_{L^2(\Omega)} \qquad \forall\, v \in H_0^1(\Omega). \tag{A.3}$$

At this point, let us interpolate estimates (A.2) and (A.3), getting

$$\|v\|_{L^2(\Omega \setminus \overline{\Omega}_1)} \leq C h_{\max}^s \|v\|_{H_i^s(\Omega)} \qquad \forall\, v \in H_i^s(\Omega). \tag{A.4}$$

∎

Acknowledgements. We would like to thank Pablo Antolín who provided us a tool to perform integration on trimmed geometries in GeoPDEs. We thank for funding the ERC AdG project CHANGE n. 694515, the MIUR PRIN project "Metodologie innovative nella modellistica differenziale numerica", along with Istituto Nazionale di Alta Matematica (INdAM).

REFERENCES

[1] A. Aimi, F. Calabrò, M. Diligenti, M. L. Sampoli, G. Sangalli, and A. Sestini, *Efficient assembly based on B-spline tailored quadrature rules for the IgA-SGBEM*, Comput. Methods Appl. Mech. Engrg., 331 (2018), pp. 327–342, https://doi.org/10.1016/j.cma.2017.11.031.

[2] P. Antolín, A. Buffa, and M. Martinelli, *Isogeometric Analysis on Vrep: first results*. In preparation.

[3] Y. Bazilevs, L. Beirão da Veiga, J. A. Cottrell, T. J. R. Hughes, and G. Sangalli, *Isogeometric analysis: approximation, stability and error estimates for h-refined meshes*, Mathematical Models and Methods in Applied Sciences, 16 (2006), pp. 1031–1090.

[4] L. Beirão da Veiga, A. Buffa, G. Sangalli, and R. Vázquez, *Mathematical analysis of variational isogeometric methods*, Acta Numerica, 23 (2014), pp. 157–287.

[5] C. Bracco, A. Buffa, C. Giannelli, and R. Vázquez, *Adaptive isogeometric methods with hierarchical splines: An overview*, Discrete & Continuous Dynamical Systems - A, 39 (2019), p. 241, https://doi.org/10.3934/dcds.2019010.

[6] J. H. Bramble, J. E. Pasciak, and O. Steinbach, *On the stability of the L^2 projection in $H^1(\Omega)$*, Mathematics of Computation, 71 (2002), pp. 147–156.

[7] M. Breitenberger, A. Apostolatos, B. Philipp, R. Wüchner, and K.-U. Bletzinger, *Analysis in computer aided design: Nonlinear isogeometric b-rep analysis of shell structures*, Computer Methods in Applied Mechanics and Engineering, 284 (2015), pp. 401 – 457, https://doi.org/10.1016/j.cma.2014.09.033. Isogeometric Analysis Special Issue.

[8] H. Brezis, *Functional Analysis, Sobolev Spaces and Partial Differential Equations*, Universitext, Springer New York, 2010.

[9] A. Buffa, E. M. Garau, C. Giannelli, and G. Sangalli, *On Quasi-Interpolation Operators in Spline Spaces*, Springer International Publishing, Cham, 2016, pp. 73–91.

[10] E. Burman, *Ghost penalty*, Comptes Rendus Mathematique, 348 (2010), pp. 1217 – 1220.

[11] E. Burman, S. Claus, P. Hansbo, M. G. Larson, and A. Massing, *CutFEM: Discretizing geometry and partial differential equations*, International Journal for Numerical Methods in Engineering, 104 (2015), pp. 472–501.

[12] E. Burman and P. Hansbo, *Fictitious domain finite element methods using cut elements: II. A stabilized Nitsche method*, Applied Numerical Mathematics, 62 (2012), pp. 328 – 341. Third Chilean Workshop on Numerical Analysis of Partial Differential Equations (WONAPDE 2010).

[13] E. Burman and P. Zunino, *Numerical Approximation of Large Contrast Problems with the Unfitted Nitsche Method*, Springer Berlin Heidelberg, Berlin, Heidelberg, 2012, pp. 227–282.

[14] J. A. Cottrell, T. J. R. Hughes, and Y. Bazilevs, *Isogeometric Analysis: Toward Integration of CAD and FEA*, Wiley Publishing, 1st ed., 2009.

[15] M. Dauge, A. Düster, and E. Rank, *Theoretical and Numerical Investigation of the Finite Cell Method*, Journal of Scientific Computing, 65 (2015), pp. 1039–1064.

[16] F. de Prenter, C. Lehrenfeld, and A. Massing, *A note on the stability parameter in Nitsche's method for unfitted boundary value problems*, Computers and Mathematics with Applications, 75 (2018), pp. 4322 – 4336.

[17] F. de Prenter, C. Verhoosel, G. van Zwieten, and E. van Brummelen, *Condition number analysis and preconditioning of the finite cell method*, Computer Methods in Applied Mechanics and Engineering, 316 (2017), pp. 297 – 327. Special Issue on Isogeometric Analysis: Progress and Challenges.

[18] A. Embar, J. Dolbow, and I. Harari, *Imposing Dirichlet boundary conditions with Nitsche's method and spline-based finite elements*, International Journal for Numerical Methods in Engineering, 83 (2010), pp. 877–898.

[19] S. Fernández-Méndez and A. Huerta, *Imposing essential boundary conditions in mesh-free methods*, Computer Methods in Applied Mechanics and Engineering, 193 (2004), pp. 1257 – 1275. Meshfree Methods: Recent Advances and New Applications.

[20] M. Fournié and A. Lozinski, *Stability and Optimal Convergence of Unfitted Extended Finite Element Methods with Lagrange Multipliers for the Stokes Equations*, in Geometrically Unfitted Finite Element Methods and Applications, S. P. A. Bordas, E. Burman, M. G. Larson, and M. A. Olshanskii, eds., Springer International Publishing, 2017, pp. 143–182.

[21] A. Hansbo and P. Hansbo, *An unfitted finite element method, based on Nitsche's method, for elliptic interface problems*, Computer Methods in Applied Mechanics and Engineering, 191 (2002), pp. 5537–5552.

[22] J. Haslinger and Y. Renard, *A New Fictitious Domain Approach Inspired by the Extended Finite Element Method*, SIAM Journal on Numerical Analysis, 47 (2009), pp. 1474–1499.

[23] K. Höllig, U. Reif, and J. Wipper, *Weighted Extended B-Spline Approximation of Dirichlet Problems*, SIAM Journal on Numerical Analysis, 39 (2001), pp. 442–462.

[24] T. J. R. Hughes, *Isogeometric analysis: Progress and challenges*, Comput. Methods Appl. Mech. Engrg., 316 (2017), pp. 1–1269, https://doi.org/10.1016/j.cma.2016.12.027. (special issue).

[25] T. J. R. Hughes, J. A. Cottrell, and Y. Bazilevs, *Isogeometric analysis: CAD, finite elements, NURBS, exact geometry and mesh refinement*, Computer Methods in Applied Mechanics and Engineering, 194 (2005), pp. 4135 – 4195.

[26] T. Jonsson, M. G. Larson, and K. Larsson, *Graded Parametric CutFEM and CutIGA for Elliptic Boundary Value Problems in Domains with Corners*, 2018, https://arxiv.org/abs/arXiv:1812.08568.

[27] A. J. Lew and M. Negri, *Optimal convergence of a discontinuous-Galerkin-based immersed boundary method*, ESAIM: Mathematical Modelling and Numerical Analysis, 45 (2011), pp. 651–674.

[28] B. Marussig, R. Hiemstra, and T. J. R. Hughes, *Improved conditioning of isogeometric analysis matrices for trimmed geometries*, Computer Methods in Applied Mechanics and Engineering, 334 (2018), pp. 79 – 110.

[29] B. Marussig and T. J. R. Hughes, *A Review of Trimming in Isogeometric Analysis: Challenges, Data Exchange and Simulation Aspects*, Archives of Computational Methods in Engineering, (2017).

[30] F. Massarwi and G. Elber, *A B-spline Based Framework for Volumetric Object Modeling*, Comput. Aided Des., 78 (2016), pp. 36–47, https://doi.org/10.1016/j.cad.2016.05.003.

[31] A. P. Nagy and D. J. Benson, *On the numerical integration of trimmed isogeometric elements*, Computer Methods in Applied Mechanics and Engineering, 284 (2015), pp. 165 – 185, https://doi.org/10.1016/j.cma.2014.08.002. Isogeometric Analysis Special Issue.

[32] B. Philipp, M. Breitenberger, I. D'Auria, R. Wüchner, and K.-U. Bletzinger, *Integrated design and analysis of structural membranes using the isogeometric b-rep analysis*, Computer Methods in Applied Mechanics and Engineering, 303 (2016), pp. 312 – 340, https://doi.org/10.1016/j.cma.2016.02.003.

[33] L. A. Piegl, *Ten challenges in computer-aided design*, Computer-Aided Design, 37 (2005), pp. 461–470, https://doi.org/10.1016/j.cad.2004.08.012.

[34] A. Quarteroni and A. Valli, *Numerical Approximation of Partial Differential Equations*, Springer Berlin Heidelberg, 1994.

[35] E. Rank, M. Ruess, S. Kollmannsberger, D. Schillinger, and A. Düster, *Geometric modeling, isogeometric analysis and the finite cell method*, Computer Methods in Applied Mechanics and Engineering, 249-252 (2012), pp. 104 – 115. Higher Order Finite Element and Isogeometric Methods.

[36] R. F. Riesenfeld, R. Haimes, and E. Cohen, *Initiating a CAD renaissance: multidisciplinary analysis driven design: framework for a new generation of advanced computational design, engineering and manufacturing environments*, Comput. Methods Appl. Mech. Engrg., 284 (2015), pp. 1054–1072, https://doi.org/10.1016/j.cma.2014.11.024.

[37] G. Sangalli and M. Tani, *Matrix-free weighted quadrature for a computationally efficient isogeometric k-method*, Comput. Methods Appl. Mech. Engrg., 338 (2018), pp. 117–133, https://doi.org/10.1016/j.cma.2018.04.029.

[38] D. Schillinger, L. Dedè, M. A. Scott, J. A. Evans, M. J. Borden, E. Rank, and T. J. R. Hughes, *An isogeometric design-through-analysis methodology based on adaptive hierarchical refinement of NURBS, immersed boundary methods, and T-spline CAD surfaces*, Comput. Methods Appl. Mech. Engrg., 249/252 (2012), pp. 116–150, https://doi.org/10.1016/j.cma.2012.03.017.

[39] R. Stenberg, *On some techniques for approximating boundary conditions in the finite element method*, Journal of Computational and Applied Mathematics, 63 (1995), pp. 139 – 148. Proceedings of the International Symposium on Mathematical Modelling and Computational Methods Modelling 94.

[40] I. Stroud, *Boundary Representation Modelling Techniques*, Springer London, 2006, http://dx.doi.org/10.1007/978-1-84628-616-2.

[41] L. Tartar, *An Introduction to Sobolev Spaces and Interpolation Spaces*, Springer-Verlag Berlin Heidelberg, 2007.

[42] R. Vázquez, *A new design for the implementation of isogeometric analysis in Octave and Matlab: GeoPDEs 3.0*, Computers and Mathematics with Applications, 72 (2016), pp. 523 – 554.

[43] Y. Wang, D. J. Benson, and A. P. Nagy, *A multi-patch nonsingular isogeometric boundary element method using trimmed elements*, Computational Mechanics, 56 (2015), pp. 173–191, https://doi.org/10.1007/s00466-015-1165-y.

[44] B. Wassermann, S. Kollmannsberger, T. Bog, and E. Rank, *From geometric design to numerical analysis: a direct approach using the finite cell method on constructive solid geometry*, Comput. Math. Appl., 74 (2017), pp. 1703–1726, https://doi.org/10.1016/j.camwa.2017.01.027.

Recent publications:

INSTITUTE of MATHEMATICS
MATHICSE Group

Ecole Polytechnique Fédérale (EPFL)

CH-1015 Lausanne

2019

01.2019 ASSYR ABDULLE, DOGHONAY ARJMAND, EDOARDO PAGANONI
Exponential decay of the resonance error in numerical homogenization via parabolic and elliptic cell problems

02.2019 CESARE BRACCO, CARLOTTA GIANNELLI, MARIO KAPL, RAFAEL VÁZQUEZ
Isogeometric analysis with C1 hierarchical functions on planar two-patch geometries

03.2019 SOPHIE HAUTPHENNE, STEFANO MASSEI
A low-rank technique for computing the quasi-stationary distribution of subcritical Galton-Watson processes

04.2019 ALESSIA PATTONA, JOHN-ERIC DUFOUR, PABLO ANTOLIN, ALESSANDRO REALI,
Fast and accurate elastic analysis of laminated composite plates via isogeometric collocation and an equilibrium-based stress recovery approach

05.2019 ALICE CORTINOVIS, DANIEL KRESSNER, STEFANO MASSEI
On maximum volume submatrices and cross approximation for symmetric semidefinite and diagonally dominant matrices

06.2019 ANNALISA BUFFA, RICCARDO PUPPI, RAFAEL VAZQUEZ
A minimal stabilization procedure for isogeometric methods on trimmed geometries

***